Diagnostics and control for the steady state and pulsed tokamak DEMO

2016 Nucl. Fusion 56 026009

(http://iopscience.iop.org/0029-5515/56/2/026009)

IOP Publishing | International Atomic Energy Agency Nuclear Fusion

Nucl. Fusion **56** (2016) 026009 (23pp) doi:10.1088/0029-5515/56/2/026009

Diagnostics and control for the steady state and pulsed tokamak DEMO

F.P. Orsitto[1], R. Villari[1], F. Moro[1], T.N. Todd[2], S. Lilley[2], I. Jenkins[2], R. Felton[2], W. Biel[3], A. Silva[4], M. Scholz[5], J. Rzadkiewicz[9], I. Duran[6], M. Tardocchi[7], G. Gorini[7], C. Morlock[8], G. Federici[8] and A. Litnovsky[10]

[1] ENEA for EUROfusion, via E. Fermi 45, 00040 Frascati (Roma), Italy
[2] CCFE Culham Science Centre Abingdon OX14 3DB(UK)
[3] Institute of Energy and Climate Research, FZ Julich Gmbh, D-52425 Julich, Germany
[4] Instituto de Plasmas e Fusão Nuclear, Instituto Superior Técnico, Universidade de Lisboa, 1049-001 Lisboa, Portugal
[5] Henryk Niewodniczański Institute of Nuclear Physics, PAN, Kraków, Poland
[6] Institute of Plasma Physics AS CR, Za Slovankou 3, 182 00 Praha 8, Czech Republic
[7] Istituto di Fisica del Plasma CNR, Via Roberto Cozzi, 53,20125 Milano, Italy
[8] Eurofusion Project Management Unit, Boltzmannstr. 2, 85748 Garching, Germany
[9] National Centre for Nuclear Research, 05-400 Otwock, Poland
[10] Institut für Plasmaphysik, Forschungszentrum Jülich, D-42425 Jülich, Germany

E-mail: Francesco.Orsitto@enea.it and fporsitto@gmail.com

Received 19 December 2014, revised 17 November 2015
Accepted for publication 18 November 2015
Published 15 January 2016

Abstract

The present paper is devoted to a first assessment of the DEMO diagnostics systems and controls in the context of pulsed and steady state reactor design under study in Europe. In particular, the main arguments treated are: (i) The quantities to be measured in DEMO and the requirements for the measurements; (ii) the present capability of the diagnostic and control technology, determining the most urgent gaps, and (iii) the program and strategy of the research and development (R&D) needed to fill the gaps. Burn control, magnetohydrodynamic stability, and basic machine protection require improvements to the ITER technology, and moderated efforts in R&D can be dedicated to infrared diagnostics (reflectometry, electron cyclotron emission, polarimetry) and neutron diagnostics. Metallic Hall sensors appear to be a promising candidate for magnetic measurements in the high neutron fluence and long/steady state discharges of DEMO.

Keywords: measurement systems, fusion reactor, fusion plasma diagnostics

(Some figures may appear in colour only in the online journal)

1. Introduction

The study of a credible design point for a DEMO device [1] is devoted to the demonstration of the capability of a tokamak-based fusion reactor to deliver electricity to the grid. The assessment of the concrete possibility of an efficient control of the main parameters of the plasma scenario and the determination of the technical figures of the subsystems are essential parts of this study. This control has the aim of protecting the device and investment made for producing energy. In this sense, the study of the diagnostics (intended as sensors) and the controls of the important quantities related to plasma stability, together with the instruments and measurement technology, make up a crucial chapter of DEMO design [2]: The diagnostics are dedicated to the protection of the device and to guarantee that the efficiency of the fusion process is kept at the best design point. The diagnostics design is therefore embedded in the engineering and physics design of a DEMO device. The present paper is devoted to a first assessment (made in the context of the EU power plant programme) of DEMO diagnostics systems and controls. In particular, the questions to be answered are: (i) What quantities need to be measured in the DEMO and the requirements for the measurements; (ii) what is the present capability of the diagnostic and

control technology, determining the most urgent gaps and (iii) the program of R&D needed to fill the gaps. The plan of this paper is as follows: In section 2, a short overview of the DEMO design parameters for both pulsed and steady state devices is given; in section 3 the DEMO environment is defined in terms of neutron fluences, a recent neutronic analysis is presented, and the consequences of the installation of the sensors are outlined; in section 4, the arguments are developed on the diagnostics and control needs of a DEMO device, a strategy for their development, and a strategy for machine protection are also outlined; in section 5, the technical specifications and diagnostics systems for the burn control are discussed; in section 6, the essential measurements and candidate diagnostics for the DEMO are listed and a gap analysis is presented; in section 7, a short summary and conclusions are presented. The results presented in this paper are obtained in the context of an EFDA (European fusion development agreement) task on DEMO diagnostics and instrumentation [3] and some partial results reported at the 'Fusion Reactor Diagnostics' Conference, Varenna 2013 [4]. The word DEMO is used when a generic fusion reactor demonstrative device is considered; DEMO1 refers to the pulsed reactor model, and DEMO2 to the steady state model.

2. DEMO reference parameters

The reference DEMO reactor tokamak concepts developed over the years are related to pulsed and steady state models [1]. The engineering and technical challenges of the models are different, mainly connected to the physics scenario used for the reactor. The pulsed reactor (DEMO1) works using a basic H-mode scenario, and the current is driven inductively by the central solenoid; the heating and current drive system(s) are devoted to keeping the plasma at a high temperature and density (Neutral Beams) and stabilizing the MHD modes (ECRH, Electron Cyclotron Resonance Heating). The plasma parameters are obtained by extrapolating the currently known scaling laws of energy confinement [5]. The typical dimensionless parameters are $q_{95} = 3$, $\beta_N \sim 2$, n/nG ~ 1.2 (n is the plasma density and nG the Greenwald density), HHy2 ~ 1–1.1 (the improvement confinement factor using the IPBy2 scaling law), and $Q =$ Pfus/Padd $= 36$.

Table 1 reports an example of a DEMO1 [6] set of parameters compared to the ITER H-mode baseline [7]. The main differences between ITER and DEMO1 are the major radius, fusion power, aspect ratio, neutron wall load, neutron fluence, and pulse length. The working point at 20% over the Greenwald density limit is a characteristic of this DEMO1 model, which together with the increase (with respect to ITER) in major radius and aspect ratio brings the fusion power to 1.7GW. The DEMO1 plasma is characterized by a value of the ratio between the alpha power and the external additional heating P_α/Pext.heat ~ 7: The alpha heating is the main heating tool (burning plasma), while in ITER P_α/Pext.heat ~ 2. The additional heating is composed of neutral beam injection (NBI) (1MeV beams), and ECRH.

A steady state device is based on the advanced tokamak concept that takes profit from the improved confinement properties of the discharged with shear reversed or flat q-profile and on the high fraction of bootstrap current (fbs $\geqslant$ 40%), so a fraction $\geqslant$ 50% of plasma current is supplied by the current drive systems.

Table 1. DEMO models compared with the ITER baseline and steady state.

Table 1	ITER	DEMO1	ITER SS	DEMO2
Major radius R0 (m)	6.2	9	6.35	8.5
Minor radius a (m)	2	2.38	1.85	2.833
Aspect ratio A	3.1	3.78	3.43	3
Magnetic field (T)	5.3	6.64	5.18	5.815
Plasma current Ip (MA)	15	15.6	9	23.33
Fusion output (MW)	400	1793	356	2.500
Fusion gain (Q)	10	36	5.7	12
Heating power (α + external)(MW)	120	409	130	455
Current DRIVE power (MW)	0	0	59.	206
Confinement improvement factor HHy2	1	1.1	1.57	1.3
Norm Beta βN	1.56	2.3	2.95	3.49
Bootstrap fraction fbs = Ibs/Ip	0.22	0.374	0.48	0.4
Normalized density ne/nG	0.85	1.2	0.82	0.845
Neutron wall load (MW m^{-2})	0.5	1.148	0.4	1.384
Pulse length (h)	0.11	1.83	0.83	277

The parameters for a steady state (SS) device (DEMO2) are given in table 1 together with ITER SS at $Q = 5.7$. The differences between ITER SS and DEMO2 are the major radius, the aspect ratio, the plasma current Ip, the normalized beta, and the fusion power. The necessity of ensuring the MHD stability (and its link to the confinement properties) of DEMO2 plasma implies the controls of the pressure and current profile, which are additional needs with respect to DEMO1 (see sections 4 and 5). The current profile (in DEMO2) is dependent on the bootstrap current, which follows the pressure profile; the plasma current driven by the external CD systems must be precisely tailored (and controlled) to get the q-profile optimized for the stability and confinement.

In general, The DEMO reactor being a DEMO-nstrative device has the following important characteristics (*common to both pulsed and steady state models*) [24]:

1. Due to TBR (the Tritium Breeding ratio) >1 the space available for diagnostics [8, 9] is likely < 5 m^2
2. Radiation: P_{rad} /(P_{alpha} +$P_{Heating}$) >~ 75%; $P_{rad} = P_{br} + P_{Syn} + P_{linecore}$ (bremsstrahlung + synchrotron + line radiation from impurities in plasma core)
3. Wall material /Divertor: Metal Tungsten (ITER: Be/W)
4. Neutron fluence: ≈30–50 times ITER Fluence (ITER 0.3–0.5 MWa m^{-2};DEMO ≈ 15MWa m^{-2};1MWa m^{-2} = 4.6 10^{23} n m^{-2})
5. $P_{alpha}/P_{heating}$ >2 (7(DEMO1); 2.4(DEMO2)).

3. Environmental constraints in DEMO1: Fluences, damage, space for diagnostics

The possibility of installing diagnostics on DEMO1 is limited by i) the neutron fluence and the related damage (in dpa = displacement per atom) produced on the diagnostics components,

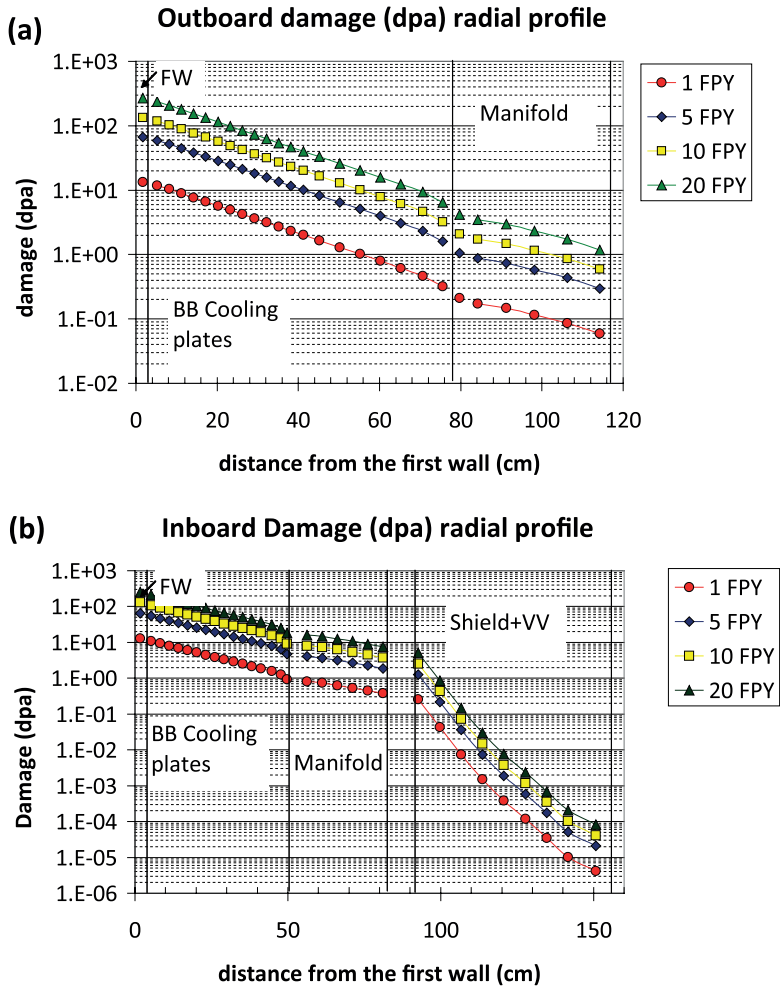

Figure 1. (a). Calculation of the outboard damage radial profile for DEMO1 for 1 to 20 full power years. (b). Calculation of the inboard damage radial profile for DEMO1 For 1 to 20 full power years.

and ii) the TBR (tritium breeding ratio): In practice the space available for diagnostics (and heating) systems is severely limited by the blanket modules to achieve a TBR > 1. In the following neutronics calculations are reported for determining the damage versus the distance from plasma on diagnostics components such as the tungsten first mirror, which can be used for infrared diagnostics (see section 5). In figure 1(a) the outboard (low field side) radial radiation damage profile calculated for DEMO1 on EUROFER steel is shown: In 1 Full Power Year (FPY) a damage of 15 dpa is produced on the first wall (FW), 1dpa at 50 cm from the FW, and about 0.1dpa at a distance of 100 cm from the FW. Similar damage is found for inboard (high field side) structures (see figure 1(b)).

From figure 1 the following data are extracted: (i) The damage in dpa corresponding to the ITER lifetime (dpa $= 3$) is reached at about a distance of 80 cm from the first wall in *ten years* of DEMO operations, in the equatorial outboard port; (ii) the damage in dpa corresponding to the ITER lifetime (dpa $= 3$) is reached at about a distance of 0.3 m from the first wall in *one year* of DEMO operations, in the equatorial inboard port.

The radial build-up of the structures considered in the calculations is given in table 2.

In these structures EUROFER and SS316 steels are used together with a tungsten first wall. The calculations are done using a Monte Carlo code with a three-dimensional (3D) structure model included, see [10, 12].

EUROFER is a reduced activation ferritic/martensitic steel developed in the EU as candidate structural material for fusion reactors: The composition and properties of EUROFER are given in [11].

The poloidal distribution of the neutron flux, reported in [10] shows that there is a decrease of 45% of neutron flux going from the equatorial (neutron flux 1,82 MW m^{-2}) to the vertical port (neutron flux 1 MW m^{-2}). The possibility of installing diagnostics away from the outboard equatorial plane is then considered for two reasons: (i) More space available left by the blanket modules; (ii) less neutron flux and damage likely 45% less that on the outboard equatorial plane.

Now, moving on to the determination of a candidate first mirror for DEMO, we note that the recrystallized tungsten (rcW) mirror [13] is considered as a candidate for the ITER first mirror. In particular, for the interferometry–polarimetry and for the electron cyclotron emission diagnostics the use of tungsten first plasma-viewing mirrors is considered to be a suitable option. Presently, tungsten is considered one of the

Table 2. Radial build-up of structures considered in neutronics calculations and their material compositions for DEMO1.

Component	Inboard thickness (mm)	Outboard thickness (mm)	Material composition
First wall (FW) armor	2	2	W
FW	30	30	Eurofer 63.5%, He 37.5%
Breeding zone	475	775	Eurofer 51%, He 49%
Cooling plates	6.5	6.5	Eurofer 57.6%, He 42.4%
Stiffening plates	11	11	Pb-15.8Li, 90% ^{6}Li
Breeder material	475	775	
Manifold	300	400	LiPb 5%, Eurofer 28%, He 67%
Shielding	300	400	WC 65%, Eurofer 10%, H_2O 25%
VV (vacuum vessel)	350	800	SS316 61%, H_2O 37%, B 2%
TF casing	60		SS316

Table 3. Controls for machine protection (ECRH, NBI electron cyclotron, and neutral beam heating systems, in red diagnostics where strong R&D is needed).

Control	Actuator	Sensor	Physical quantity
Disruption	ECRH, impurity gas injection, pellet, disruption mitigation system	Magnetics (Halo sensors in the blanket), reflectometry, ECE, visible and IR cameras, bolometers	Plasma current, temperature and density, heat load on divertor and wall, impurity influx
Runaway electrons	Gas injection valves, impurity gas injection, disruption mitigation system	Hard x-ray monitors, IR cameras	runaway density, divertor and wall heat load
Heat loads (divertor)	NBI, impurity gas injection, impurity pellet	Interferometry/polarimetry, bolometers, divertor tile thermocurrent and voltage	Divertors and wall heat load
Density control	Gas injection valves, pellet, NBI	Interferometry/polarimetry, reflectometry	Electron density
Plasma position	Poloidal field coils	Magnetics, reflectometry, ECE	Plasma position equilibrium
Fusion power	Gas injection valves, pellet, impurity seeding	Neutron cameras, fission chambers, neutron spectroscopy, ECE	Density, D/T ratio, temperature, dilution
Core radiation	Impurity seeding, impurity pellet	Bolometers, x-ray spectrometers, IR cameras	X and IR radiation flux
Erosion and dust	Dust collection by remote handling	In vessel viewing systems	Layers eroded and dust production
Tritium retention and removal	Glow discharges, baking of vacuum vessel	Residual gas analyzers, laser-induced ablation spectroscopy	Tritium inventory
Equilibria/MHD stability	Poloidal field coils ECRH, NBI	magnetics, polarimetry/interferometry	Magnetic flux, current profile

Table 4. Minimum set of diagnostics for machine protection.

Minimum set of diagnostics for machine protection (R&D)
Magnetics (Hall sensors to be tested at high dpa >3)
IR Cameras (W or Mo mirrors to be tested for dpa >3)
Polarimetry (W or Mo mirrors to be tested for dpa >3)
Position reflectometry (ITER reflectometry to be qualified)
Fission chambers (ITER sensors to be qualified)
X-ray spectroscopy (x-ray mirrors to be tested)
VUV and Vis spectroscopy (W or Mo mirrors)

main candidate plasma-facing materials in the current DEMO design (see also table 2); therefore, the introduction of tungsten mirrors to the DEMO will not change the set of used materials. The reflectivity of tungsten at longer wavelengths in the IR range is about 80% [14], and the optical performance of diagnostic mirrors at these wavelengths is less sensitive to adverse effects such as erosion of the mirror surface or deposition of impurities [15]. Finally, dedicated tests have proven the resistance of tungsten mirrors under neutron irradiation up to a dose of 3 dpa [13]. All these factors make tungsten an attractive candidate material choice for the first mirrors in the DEMO. The possibility of using first mirrors of rcW for the infrared wavelengths, makes realistic the option of including in DEMO1 interferometry–polarimetry and Electron Cyclotron Emission diagnostics for measuring electron temperature, density, and for equilibrium reconstruction. Is it possible in principle to use a tungsten mirror in the DEMO environment?

The plots in figures 1(a) and (b) show that in 1FPY damage of ≈15dpa is produced on the tungsten first wall, under the irradiation of a neutron flux ≈2 10^{28} n $year^{-1}$. Let us examine the possibility of placing a tungsten mirror (diameter 5 cm, thickness 2 cm, rcW) in a tube, say, with a diameter of 10 cm, viewing the plasma on the equatorial plane. The distance from the first wall is determined by the condition that the neutron flux reaching the tungsten mirror at that distance produces damage of 3dpa. In determining that distance, we can suppose that the neutrons are isotropically emitted in a large region of the equatorial plane and that the neutron source can be placed in the plasma center. Since the damage of 3dpa is 20% of 15dpa and the damage is proportional to the neutron flux, the position allowed is where the neutron flux is approximately 20% of the first wall flux. At a distance x from the first wall along the major radius, the neutron collection solid angle

Table 5. Basic control (ECRH, NBI electron cyclotron and neutral beam heating systems; NTM Neoclassical Tearing Modes; RWM Resistive Wall Modes).

Basic control	Actuator	Sensor	Physical quantity
Burn control	Impurity injection valve, gas valves, ECRH, NBI, pellet	Polarimetry/interferometry, neutron camera, neutron spectroscopy, Neutral Particle analyzers, ECE, bolometers	Electron temperature, density, D/T ratio, dilution, impurity content, ion temperature, radiation, fusion power
MHD control (NTM, RWM)	ECRH, pellet ELM pacing, NBI	Magnetics, polarimetry/interferometry neutron cameras, ECE, x-ray spectroscopy	Electron temperature, density, dilution, impurity content, rotation
Divertor control	Gas valves, impurity seeding	bolometry, polarimetry/interferometry vis and IR cameras	Heat load, detachment, plasma density, neutral density
ELM mitigation	Gas valves, pellet ELM pacing	Reflectometry, polarimetry/interferometry, ECE, bolometry, magnetics, vis spectroscopy	Pedestal pressure, MHD modes
Radiation control	Impurity injection valve, gas valves, ECRH, NBI, pellet	Bolometry, polarimetry/interferometry, IR cameras	Flux of radiation in near IR

Table 6. Advanced control (ECRH and NBI electron cyclotron and neutral beam heating systems).

Control	Actuator	Sensor	Physical quantity
Alpha heating	NBI, gas valves, ECRH, impurity gas injection	Gamma ray spectroscopy, NPA, ECE, interferometry/polarimetry, Thomson Scattering, x-ray spectroscopy, neutronics	Electron temperature, density, D/T ratio, dilution, impurity content, ion temperature, alpha particle measurements (energy distribution function and spatial profiles)
Current profile	NBI, ECRH, impurity gas injection	Interferometry/polarimetry, reflectometry, magnetics, Thomson scattering	Plasma current and pressure profile (ion and electron pressure)
Kinetic profile	Gas valves, NBI, ECRH, pellet, pellet ELM pacing	ECE, interferometry/polarimetry, neutron camera, Thomson scattering	Plasma pressure profile (ion and electron pressure)

subtended by the mirror will be of the order $\Omega_2 = \frac{\pi * D^2}{(4 * (a+x)^2)}$, where D is the mirror diameter and a is the minor radius of the torus. The position x is determined by the condition that $\Omega_2 = 0.2 * \frac{\pi * D^2}{(4 * a^2)}$, i.e. $x = 1.236*2.38 = 2.94$ m. Placing a first mirror of tungsten in a tube viewing plasma at ≈3 m from the first wall can be useful for 1FPY of DEMO operation.

4. Strategy for DEMO diagnostics and control development

4.1. DEMO operational planning

The operational planning of the DEMO (pulsed and steady state) can consider two phases [3, 6], the ITER-like phase (ILP) and the power-plant phase (PPP). The ILP is a preparatory and commissioning period, where the scenario and the subsystems are progressively brought to the device operating point. In the ILP the main achievement would be the implementation of the burn-control in a condition where $P_{alpha}/P_{input} > 2$. In this context, the realization of the full control of the machine using a reduced set of diagnostics will be implemented by physics-based control codes, which include a physical model of the scenario complemented by the measurements of a reduced set of diagnostics [16]. For this purpose, i.e. to obtain/test a precise physics model of the scenario to be included in the control code, the ILP will have an extensive set (compatible with the space available) of ITER-like diagnostics, in particular profile diagnostics. The power-plant phase will include the operation where the TBR (Tritium breeding ratio) >1 [9] is realized, and only the reduced set of diagnostics can be used for the control of the scenario and machine protection to maximize the space available for the blanket.

4.2. DEMO control needs

The control needs for the DEMO can be divided into three classes: (i) Machine protection, (ii) basic control, and (iii) advanced control. This classification is on the basis of the ITER diagnostics and control systems [17], with important changes: (i) The class related to the physics studies (used for ITER) is not included in the DEMO control; (ii) the advanced control will be operated only in the ILP for the burn control and physics model implementation of control codes. In practice, the control needs for the DEMO are limited to machine protection and basic control. Tables 3–6 give an overview of the control needs of a fusion reactor according to this classification. The advanced control implies the use of diagnostics likely not surviving during the power plant phase will be very useful in the ILP. The tables also broadly follow the classification made for ITER plasma control [18], but are adapted to DEMO sensor and actuator availability.

4.2.1. Control of machine protection (table 3). The machine protection control is dedicated to preventing machine damage by (i) disruption and sudden loss of control of the heat loads on the divertor and wall, runaway electrons generation and mitigation, (ii) fusion power instability and alpha particle

loss due to interaction with the MHD modes. The control tools and their margins are critical because the control by the heating systems is marginal (since $P_{alpha}/P_{input} > 2$), so the pellet edge localized modes (ELM) pacing, impurity, and density control play an important role. The other important issue is the radiation control (see also section 2), which is typical of the DEMO, as it is the only way to mitigate the divertor damage through the divertor detachment [19, 24]. The role of the reduced set of diagnostics (see section 5) in this context is outlined in table 3, where diagnostics systems are shown in red, where at the moment the extrapolation of the ITER technology to DEMO seems particularly demanding: Bolometers, x-ray cameras, and spectrometers need to be developed for the DEMO, as well as divertor tile thermocurrent and voltage sensors used for divertor detachment successfully tested on ASDEX [19]. Regarding machine protection and engineering constraints, a detailed analysis is reported in [9, 20]. The minimum set of diagnostics for machine protection is detailed in table 4 The R&D needed is specified also in this table: (i) The first mirror test for W at DEMO fluences, as well as (ii) bolometer prototypes, (iii) fission chambers, and (iv) the extension to DEMO of ITER reflectometers for plasma position.

4.2.1.1. The control of a power plant and diagnostics needs: technical guidelines for machine protection in high-performance devices. The plasma-related machine protection [20] issues involve the measurement and control of plasma stability, plasma purity, and plasma-wall interactions. Machine protection aims to avoid hitting catastrophic limits by using early warning alarm systems, and controlled termination or avoidance, involving coordinated actions of the magnets, and gas and auxiliary heating or current-drive systems in high-density plasma with high radiation fraction (see section 2). In this context, key measurements are the plasma density and temperature, magnetic fluxes, neutron fluxes (see table 3). In particular, the measurements related to plasma magnetic stability and plasma density meet concrete implementation difficulties.

Plasma position and shape on the DEMO must ensure that the plasma is where it should be in relation to the plasma-facing components. The equilibrium reconstruction is done using the measurements produced by magnetic pick-up coils (together with polarimetry/interferometry), which necessarily must be mounted *behind the blanket modules*. The effects induced by neutrons on cables and sensors already documented for the ITER will be mitigated in this position. The blanket's functional and structural materials would screen the magnetic fields, so the control must be designed and operated mindful of a systemic *time delay*. The candidate magnetic sensors are the metallic Hall sensors [21], which could guarantee reasonable resistance to the high neutron fluence (see section 7), and, since they are intrinsically ac, long-term drifts of the signals will be avoided.

In present-day machines, the plasma density is usually measured by interferometry/polarimetry, which yields a line-integrated density (or Thomson scattering, which yields a density profiled across the plasma cross-section). Polarimetry (through the measurement of the Cotton–Mouton effect proportional to the plasma density) provides an instantaneous value and does not suffer from the fringe jump problem (as interferometry). They require high reliability, and high power lasers, optics, and detectors. In the DEMO, these components would be located in dedicated reentrant tubes viewing the plasma beyond the neutron absorbing blanket using tungsten or molibdenum first mirrors placed in a position a few meters from the first wall: So *the mechanical stability constraints on the optical path and components must be considered.*

4.2.2. Basic and advanced controls. The basic and advanced controls are dedicated to the scenario control and include the tools for the validation of the physics-based models to be inserted in the control codes in real time: Examples are reported in [16].

The basic control in table 5 shows the main scenario control needs.

The burn control will be discussed in detail in section 5. Here comments on the remaining controls are given. The difference among control for 'fusion power' (in table 3), 'burn control' (table 5), and 'alpha heating' (table 6) are related to different aspects and progressive (moving from tables 3–6) details requested in the context of 'burn control'. In table 3 the fusion power is controlled in the context of machine protection, in practice monitors of neutron production and burn equilibrium temperature are useful and actuators aimed at the stability of the burn and safety of the device are needed. In table 5 the basic 'burn control' is treated when the various quantities entering the dependence of the equilibrium temperature (see section 5.1) and fusion power are measured. In table 6 the details of the alpha distribution function are included, these measurements are considered important in the ILP, for the calibration of the physics based control code, and will be not working in the PPP.

4.2.2.1. MHD control. The MHD control includes the neoclassical tearing modes (NTMs) and the resistive wall modes (RWMs). The RWMs will be important in DEMO2 since they are a dominant mode at high beta, while for both (DEMO1 and DEMO2) the NTM control is necessary.

The NTM control has been demonstrated in various devices using ECRH, and it can be done in real time without the equilibrium evaluation since the same optical system can be used for the ECE measurement of electron temperature profiles inferring the MHD island dynamics and for localized heating. The interaction of impurity with MHD activity is related to the local cooling of plasma due to the presence of impurities that irradiate, changing locally the resistivity and influencing the evolution of resistive instabilities like tearing modes. The impurity content (in particular the tungsten content) can be measured using VUV spectroscopy and light impurities by the visible spectroscopy.

The (limited possibility of) control of RWM by rotation can be done using beams, and measuring the plasma rotation. The possibility of the stabilization of RWM by coils (as will be done on JT60SA) mounted behind the blanket in DEMO2 need to be demonstrated (for example on JT-60SA).

4.2.2.2. Advanced control. The advanced control is the physics scenario control, which is also useful for the calibration of

Table 7. Divertor similarity parameter for AUG, ITER baseline, DEMO1.

	ITER	DEMO1	AUG
Psep/R (MW m^{-1})	15.0	15.5	7.0

the physics modules of the control codes to be used in the PPP. In table 6 the control table for this phase is reported.

The current profile is a DEMO2 control need, while the other controls are common to DEMO1 and DEMO2.

Inspecting table 6, the profile diagnostics are included in the controls. In the alpha heating the electron kinetics is measured by incoherent Thomson scattering, interferometry/ polarimetry (which can give electron density and an approximate measurement on electron temperature), and ECE (electron cyclotron emission). The ion temperature is measured by crystal x-ray spectroscopy (ion temperature) and the fast ions can be measured by the neutral particle analyzers (NPAs). The ion temperature can also be inferred by neutron profile monitors because of the strong dependence of the neutron flux on the central ion temperature and possibly by high-resolution neutron spectroscopy. Both x-ray crystal spectroscopy and NPA need a direct view to the plasma. For x-ray crystal spectroscopy the crystal can be mounted faraway from the plasma in a place where the neutron flux is strongly attenuated. For NPA the same comment can be applied, see [22] and section 5.2 for comments on the feasibility of NPA on the DEMO.

The possibility of a fast particle monitor to measure the isotopic ratio by a simplified NPA used without the energy spectrum analysis is considered feasible for the DEMO [22].

The measurement of the q-profile is important for DEMO2 since in advanced tokamak regimes both the current profile and pressure profile are controlled together because the bootstrap current (which depends on the pressure profile) is at least 40% of the total plasma current. Demonstrative experiments of the q-profile control were done on a JET using heating systems as actuators and interferometry/polarimetry as sensors [57, 58] used for the reconstruction of the equilibrium in real time.

The fast ion dynamics (including alpha particles) can be measured by gamma-ray spectroscopy, in particular for ions whose energy is higher than 1MeV: This is an integrated line integral measurement like the NPA. Neutron absorbers (for example LiH) are used in neutron profile monitoring to allow for the measurements of the gammas produced on nuclear decays [23].

4.2.3. Divertor and radiation control. The power exhaust in the DEMO models (see table 1) is identified as a critical aspect to be solved for fusion reactors [24].

The present analysis considers [24] that (i) the (time and space averaged) maximum heat flux on the divertor tiles of Pdiv $\approx$ 5–10 MW m^{-2} must be respected if a lifetime of 2FPY is considered and ii) a divertor plasma temperature Tdiv $\leqslant$ 5 eV is compatible with an acceptable erosion of the tiles.

In DEMO1 an estimation of the total power crossing the separatrix (Psep) is close to Psep = 200 MW, which leads to a power load on the divertor of the order of 140 MW m^{-2}, assuming a 'wetted' area of the divertor of the order of $A_w = 1.4m^2$. A sustainable load on the divertor is estimated around 10 MW m^{-2}, which means that a mitigation of the load on the divertor must be found. If the plasma radiated power is increased to 90% of the total separatrix power, than the power load on the divertor can be reduced to 15 MW m^{-2}, which is close to the sustainable value [19].

The similarity parameter Psep/R (R is the major radius) was introduced in [25] to compare divertor plasmas: Physically similar divertor plasmas would have the same Psep/R. The divertor control is then a critical area, and this can be realized looking into the values of the divertor similarity parameters Psep/R, as shown in table 7, where a comparison is made between the value of Psep/R obtained on the ASDEX Upgrade (AUG) [19], leading to a control of the divertor conditions below the maximum tolerable power load, and the values projected for the ITER and DEMO1.

The ITER and DEMO1 Psep/R values represent the conditions of the reactor divertors. The value of Psep/R (AUG) is presently the maximum value reached in experiments so far. The impurity seeding using Ar and N was demonstrated on AUG [19] to control the level of detachment of the divertor, to control the radiation in the outer core and divertor, and to keep the power load on the divertor to tolerable values of Psep/R $\leqslant$10 MW m^{-1}. In this case the control parameters were the divertor temperature (measured by the divertor tile thermocurrent and voltage) and the divertor radiation. *The demonstration of the divertor control in DEMO relevant conditions is considered one of the most critical points for the realization of a fusion reactor*. This means that measurements must be taken of the radiated power (measured by bolometry), the power load on the divertor (measured by the divertor tile thermocurrent and voltage), together with the impurity content (measured by visible/ VUV spectroscopy). The actuators are impurity injection valves.

4.3. Development plan for DEMO diagnostics

The development plan for the DEMO diagnostic and control system is based on top-level requirements for DEMO control, which are summarized as follows.

The DEMO main control system should: 1. Provide stable operation of the plasma and of all subsystems of the DEMO in compliance with safety requirements, specifically by strictly avoiding any safety-related accidents; 2. avoid plasma disruption and any off-normal events (risk of melting the wall); control/maximize fusion power and efficiency; control/minimize aging of the machine (e.g. erosion, cyclic loads), see section 4.2 and tables 3 and 4.

An emergency control system will provide fast shut down of the plasma and subsystems, automatically selecting a termination sequence appropriate to the problem in the event of main control system failure.

The development of DEMO diagnostics and control has to be performed according to the following main directions:

(1) Develop a DEMO-integrated control requirements table (see also table 15 and section 5), which

Table 8. DEMO space and time scales.

Symbol	Meaning	DEMO1	DEMO2
<ne> Vol	Volume average density	9,47E + 19	6,37E + 19
ne0/<ne> Vol	Peak/volume av. density	1,3	1,5
<Te> Vol(keV)	Volume average temperature	12,87	16,29
Te0/<Te> Vol	Peak/volume av. temperature	2	2,5
τE_confinem(s)	Confinement time	3,39	3,84
R0	Major radius	9	8,5
A	Aspect ratio	3,78	3
a = R0/A(m)	Minor radius	2,38	2,83
τ_DEUT _collis(s)	Collision time D-D	2,43E − 02	5,16E − 02
τ_elec_collis(s)	Collison time e-e	3,12E − 04	6,61E − 04
ρ_Tor_DEUT(m)	Toroidal deuterium larmor radius	3,50E − 03	4,50E − 03
ρ_Tor_Trit(m)	Toroidal tritium larmor radius	4,30E − 03	5,50E − 03
ρ_Tor_Alpha(m)	Toroidal alpha larmor radius	4,00E − 02	4,60E − 02
ρ_pol_proton(m)	Poloidal proton larmor radius	3,90E − 02	4,50E − 02
ρ_pol_deut(m)	Poloidal deuterium larmor radius	3,96E − 02	4,09E − 02
ρ_pol_alpha(m)	Poloidal alpha larmor radius	4,60E − 01	4,20E − 01
τ_Alfven(s)	Alfven time	4,80E − 07	3,90E − 07
τ_Resistive (h)	Resistive time	3,25E + 00	6,57E + 00
1/γ(tearing) (s)	Growth time of tearing modes	8,20E − 01	1,15E + 00

Table 9. Requirements on the measurements of the interfero-polarimeter.

Interferometer/polarimeter measurements			
Measurements	Accuracy	Range	Time resolution
Faraday rotation	0.05–0.1 deg	±30deg	1 ms
Cotton–Mouton	0.2 deg	±10deg	1 ms
Line-averaged plasma density	1%	1e18-8e20m-3	1 ms

a. serves as a guiding tool for all diagnostic/control R&D,
b. provides the interface to plasma scenario development and to the system integration unit,
c. defines limits for all relevant parameters to which the plasma scenario must be adapted.

(2) Perform quantitative precise simulations of DEMO control, including realistic accuracy and response times for the diagnostics, actuators, and plasma response, with the ultimate goal of determining the necessary boundary conditions under which the plasma scenario can be reliably controlled. These control simulations shall serve to

a. Define realistic design specifications of the diagnostics, actuators, and controllers (see tables 12–14 for examples).
b. Serve as a test bed to prepare the control modules, which may form the basis for the later integrated DEMO control system.

(3) Set up a list of candidate diagnostic systems and assess/validate their performance under DEMO conditions (see sections 5 and 6), taking into account the specific implementation on the DEMO. This validation may include CAD models (mounting position, duct, shielding etc) of the diagnostic front ends on the DEMO, simulation of diagnostic accuracy (amplitudes, time response, calibration issues) and estimation of the diagnostic lifetime (degradation). A reasonable trade-off has to be found first between the need for precise plasma control and the allowed space occupation of the diagnostic front ends and their impact on the TBR, as well as for the amount of effort to enhance the control accuracy and the impact on the overall DEMO performance (reduced control accuracy may require larger control margins against operational limits and will hence reduce fusion power). The R&D on the DEMO diagnostics may be validated by specific prototype testing, e.g. on JT-60SA and ITER.

(4) Set up a list of actuators and assess/validate their performance under DEMO conditions, taking into account the specific implementation and plasma conditions on the DEMO.

Design iterations among points 1–4 have to be performed as appropriate, in order to arrive at a coherent set of results for all elements.

5. Burn control: technical specifications and diagnostics systems

5.1. Burn power balance and dependence of fusion power on the main parameters

The fusion power main dependencies upon plasma density (n) and temperature (T) (for $T < 20$ keV), plasma dilution C_α, isotopic mixture (γ), and the profile peaking factor are given by [26]

$$P_\alpha = C_\alpha f_p f_{\mathrm{MIX}} (nT)^2 V \quad (1)$$

Table 10. Polarimetry parameters evaluated for the ITER and DEMO (see text for the symbol meaning).

	W_1	W_3	FR ψ(deg)	C-M φ(deg)	nL (m^{-3}) 10^{20}	BT	Ip	R0	a	k	λ
ITER (Hmode)	0.8	2.8	87	44	1	5.3	15	6.2	2	1.75	0.118 mm
DEMO1	1.3	3.3	95	78	1	6.64	15.6	9	2.38	1.56	0.118 mm
ITER SS	0.4	1.2	34	23	0.4	5.18	9	6.35	1.85	1.85	0.118 mm
DEMO2	1.4	4.9	140	80	1.11	5.81	23.32	8.5	2.83	1.65	0.118 mm

Table 11. Diagnostic classification system based on ITER diagnostic systems, green = primary method, yellow = possible to measure the parameter, brown = provide supplementary/related information.

Parameter	Neutron camera	Fission chamber	Activation foils	Spectrometer
Fusion power	possible to measure	primary method	supplementary	
Fusion power density	primary method	supplementary	supplementary	
Total neutron flux	possible to measure	primary method	supplementary	
1st wall fluence	supplementary	supplementary	primary method	
Fuel ratio	possible to measure			primary method
Runaway	supplementary			
MHD instabilities	supplementary			
Ion temperature distribution	possible to measure			supplementary

where
P_α = alpha power
$f_{\mathrm{MIX}} = \gamma * (1-\gamma)$;$\gamma = \frac{n_T}{n_D + n_T}$;$C_\alpha$ = dilution factor = $(1 - 2f_{\mathrm{He}} - \Sigma i\ Zi\ Fi)^2$
f_{He} = Helium Fraction = $\frac{n_{\mathrm{He}}}{ne}$;
Zi = charge of impurity i; fi = fraction of impurity $i = ni/ne$;
$n_{D(T)}$ =deuterium (tritium) density;
V = plasma volume; fp = profile peaking factor = $k/(2\nu + 1)$; k = elongation; $\nu = \nu n + \nu T$ = density + temperature peaking factors; ne = electron density.

The plasma power conduction losses as determined using the IPBy2 confinement scaling law are given by (since the confinement time $\tau E\_\mathrm{IPB}y2 = n^{-0.91}\, T^{-2.26}$) [5]:

$$\mathrm{P}_{\mathrm{conduction\_loss}}(\mathrm{W}) = \frac{nT\ V}{\tau E} = n^{1.91}\, T^{3.26} \tag{2}$$

The power balance equation is expressed by the equation:

$$P_{\mathrm{input}} = P_{\mathrm{loss}}$$

where

$$\begin{aligned} P_{\mathrm{input}} &= P_{\mathrm{alpha}} + P_{\mathrm{Add\_Heating}} + P_{\mathrm{ohmic}} \approx P_{\mathrm{alpha}} + P_{\mathrm{Add\_Heating}} \\ P_{\mathrm{loss}} &= P_{\mathrm{conduction\_loss}} + P_{\mathrm{Radiation}} \end{aligned} \tag{3}$$

where P_{loss} includes the conduction losses and the total radiation ($P_{\mathrm{Radiation}}$, in the power balance the $P_{\mathrm{Radiation}}$ considered is only the core radiation).

In equation (3), the P_{ohmic} can be neglected (being of the order of 1 MW in DEMO1), and $P_{\mathrm{Add\_Heating}} = \frac{5 * P_\alpha}{Q}$, where Q is the energy amplification factor (Q = 36 for DEMO1).

Equation 3 becomes $\left(1 + \frac{5}{Q}\right) * P_\alpha = P_{\mathrm{conduction\_loss}} + P_{\mathrm{Radiation}}$

The radiation losses are kept at the level $P_{\mathrm{Radiation}} = \mathrm{krad} * P_\alpha$ so for DEMO the power balance can be approximated by (being krad >=0.75, in section 4.2.3 krad = 90% was introduced):

$$\left(1 - \mathrm{krad} + \frac{5}{Q}\right) * P_\alpha \approx P_{\mathrm{conduction\_loss}} \tag{4}$$

Using formulas (1)–(4), we get:

$$\left(1 - \mathrm{krad} + \frac{5}{Q}\right) * C_\alpha f_p f_{\mathrm{MIX}}\ (nT)^2\ V \approx n^{1.91}\ T^{3.26} \tag{5}$$

As a consequence, the (burn) equilibrium temperature (T_{eq}) is given by:

$$T_{\mathrm{eq}} \approx \left[\left(1 - \mathrm{krad} + \frac{5}{Q}\right) * V * f_p * f_{\mathrm{MIX}} * C_\alpha\right]^{0.8} n^{0.07} \tag{6}$$

From equations (1) and (6) we can extract the following information:

(i) The equilibrium temperature depends mainly on the isotopic mix, dilution, radiation fraction, and discharge geometry, *having a slow dependence upon plasma density.*
(ii) The accuracy on the fusion power measurement is set by the neutronics (1 MW fusion = 13.55 10^{17} n s^{-1}), whose accuracy (in the measurement of the neutron flux) is of the order of 10% (extrapolating the planned ITER accuracy to the DEMO); at fixed T_{eq}, (i.e. at a fixed isotopic mix, radiation, and dilution) a change of density of 5% has the effect of changing the fusion power by at least 10%. Such changes in density can be detected if the accuracy of the density measurement is set to $\delta n/n \approx 1\%$. This accuracy is the present state of the art in interferometry/polarimetry measurements. The extrapolation of this accuracy to the DEMO must be demonstrated.

5.1.1. Space and time scales for the DEMO (pulsed and steady state) plasmas. The scales of DEMO plasmas can be useful to define the requirements of the measurements.

Table 12. Requirements for the measurements (RoM) for the diagnostics of the DEMO burning plasma (in bold ITER RoM).

Table 12	Accuracy	Space resolution (bulk plasma)[a]	Time resol(s)	Systems
T_e (bulk)	5%/**10%**	a/20 (line average)/**(a/30)**	<0.01/**10^{-4}**	ECE (polarimetry)
ne	1%/**1%**	1. Line integral 2. a/20/**(a/30)**	<0.01/**0.001**	(1) Interferometry-polarimetry, (2) Reflectometry
Pfus	10%/**10%**	Line integral	<0.01/**0.001**	Neutronics

[a] Only in the pedestal region is a spatial resolution of a/30 required.

Table 8 gives the main spatial and time scales relevant to DEMO kinetics.

The minimum spatial scale is related to the ρ_tor_DEUT (toroidal deuterium gyroradius) ≈3.5 mm, the minimum time scale is the Alfven time τ_Alfven ≈0.5 μs, while the MHD tearing mode characteristic time is τ_Tearing ≈ 0.8 s.

The spatial resolution of kinetic quantities on the pedestal must be of the order of a few poloidal gyroradius of the deuterium, δr (pedestal) = 4 cm, which is very close to a/30 (ITER required spatial resolution).

In the bulk plasma, the spatial resolution can be less (at least 1/5,1/10) than the spatial gradient of temperature and density, which is the half of the radius, so δr(bulk) ≈ a/10–a/20.

5.2. Review of the diagnostics for burn control

The measurements needed (see table 5) are:

1. Electron and ion density and temperature
2. Fusion power
3. Plasma geometry
4. Impurities
5. Radiation
6. Isotopic mix

In the following paragraphs the related measurements are examined.

5.2.1. Measurement of electron density by interferometry–polarimetry. This measurement is done by interferometry–polarimetry systems in the present day machines. In the ITER both toroidal [27] and poloidal [28] interferometer/polarimeters are planned. The experience on the toroidal interfero-polarimeter (TIP) was done on the tokamak JT-60U, where a dual wavelength (λ = 10.6 μm and 9.27 μm) CO_2 toroidal interfero-polarimeter [29] was extensively tested for the measurement of electron line integrated density using Faraday rotation. In this tangential geometry the Faraday rotation is proportional to the line-integrated electron density times the toroidal magnetic field. Therefore, once the toroidal magnetic field is known the Faraday rotation gives the electron density. The poloidal interfero-polarimeters (PoPolas) are more frequent in the use of tokamak operation, and there is extensive experience in the operation of such systems. Usually in these systems the quantities measured are the Faraday rotation (FR) and the Cotton–Mouton (CM) phase shift: The FR rotation (in this geometry) is proportional to the density times the value of the magnetic field along the line of the propagation of laser beam, in this case the poloidal magnetic field proportional to the plasma current, while the CM is the product of the toroidal magnetic field times the electron density [30]. The laser wavelength used is $\lambda \geqslant 100$ μm, to get the possibility of measuring the Cotton–Mouton phase shift with good accuracy [30]. In general these techniques produce line integral density measurements whose technical specifications are: Accuracy on the line integral electron density close to 1%; time resolution =1 ms.

The electron temperature has an effect on these measurements since the dielectric tensor depends on the electron temperature: So from these measurements an evaluation of the electron temperature can be carried out. The measurement of temperature can be extracted using an equilibrium code: An accuracy of 30% in the determination of Te was evaluated in [28].

The concrete feasibility of an interferometer/polarimeter diagnostic (TIP and PoPola) on the DEMO is linked to the possibility of using tungsten or molybdenum mirrors in recessed positions (≈3 m distance from the plasma edge). As demonstrated in section 2, tungsten mirrors are good candidates.

The PoPola is essential for the equilibrium reconstruction, in particular for DEMO2, where the q-profile (as well as the pressure profiles) is important for the control of the scenario. The ITER PoPola is under study and the possibility of mounting the retroreflectors on the high field side is considered. In the following section 5.2.1.1. parameters for a polarimetry systems for DEMO are evaluated. Taking into account the experience gained so far, the technical specifications on the interferometry/polarimetry measurements are shown in table 9.

5.2.1.1. Parameters characteristic of a poloidal polarimeter for the DEMO. The primary polarimetry measurements are: (i) Faraday rotation (=); (ii) Cotton–Mouton phase shift (φ). For small polarimetry effects, two quantities W_1 and W_3 are relevant, (being for $W_1^2 << 1$ and $W_3^2 << 1$) [30, 32]:

$$W_1 = \tan\varphi = \int n\, B_T^2\, dL \sim \text{C1} * \text{nL} * (B_T^2) * 2*a*k \quad (7)$$

$$W_3 \approx 2\psi - 2\psi_0 = \int n\, B_p\, dL \sim \text{C3} * B_p * \text{nL} * 2*a*k \quad (8)$$

Where: $\text{nL} = \frac{\int n\, dL}{L_{chord}}$; Lchord = length of the polarimeter chord.

$\text{C1} = 2.42\ 10^{-20}\ \lambda_{mm}^3$; $\text{C3} = 5.23\ 10^{-19}\ \lambda_{mm}^2$

$Bp = \frac{B_T}{(A * q_{95})}$; $q95 = \frac{(5 * B_T * R_0)}{Ip} * \left(\frac{FA}{A^2}\right) * S$;

$S = (1 + k^2(1 + 2\delta^2 – 1.2\delta^3))/2$;

$\text{FA} = (1.17 - 0.65/\text{A})/(1 - 1/\text{A}^2)^2$

$\psi_0 = \pi/4$ is the input (to the plasma) angle of the laser wave electric field with respect to the toroidal magnetic field direction.

In formulas (7)–(8) nL is the line average electron density (m-3), a is the minor radius, R_0 is the major radius, k is the elongation, δ is the triangularity, B_T is the toroidal magnetic

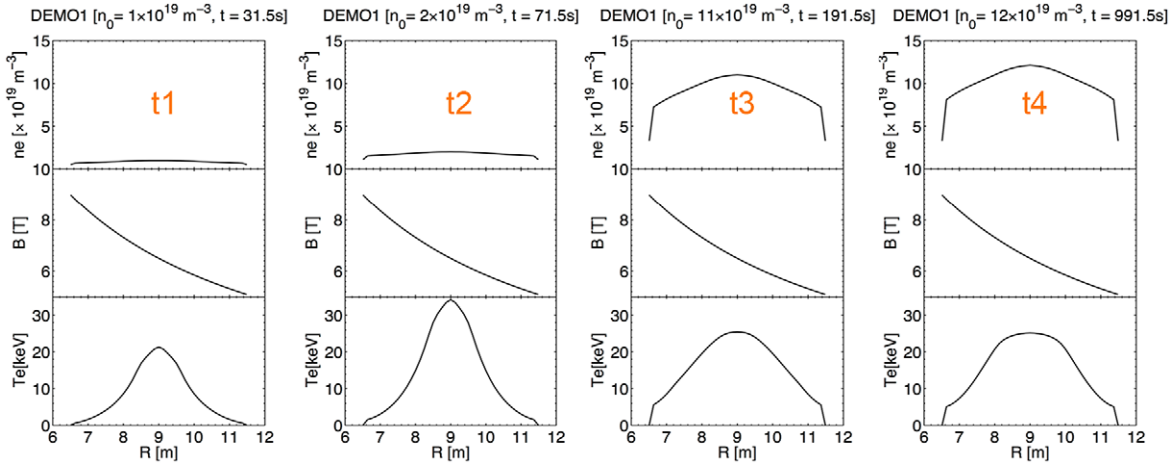

Figure 2. Density profiles, toroidal magnetic field, and temperature of DEMO1 at different times.

field on the axis, B_p is the poloidal magnetic field, C1 and C3 are the constants, λ_{mm} is the laser wavelength in millimeters, A is the aspect ratio = R/a, and q_{95} is the safety factor at 95% of the poloidal flux. The integrals in (7), (8) are intended as an integral along the beam path into the plasma (Lchord).

In equation (7), the Cotton–Mouton is proportional to the line average density, and the Faraday rotation is proportional to the line integral of the plasma density times the average poloidal magnetic field.

The polarimetry measurements (ψ and φ) can be used coupled to an equilibrium code to determine: (i) The plasma density and (ii) the plasma q-profiles. In the approximation of small effects ($W_1^2 << 1$ and $W_3^2 << 1$), the Cotton–Mouton gives the line average plasma density (once the toroidal magnetic field is known).

Table 10 reports the polarimetry quantities calculated using formulas (7)–(8) (first and second columns from the left) for the ITER and DEMO parameters, and the Faraday rotation and Cotton–Mouton resulting from the integration of the Stokes equations of the propagation of the beam polarization inside the plasma (third and fourth columns from the left) [30, 32]. The quantities are calculated for a central vertical chord with radial coordinate $R = R0 + a/3$.

In table 10, it is shown that in general the approximations for small effects ($W_1^2 << 1$ and $W_3^2 << 1$) are not applicable for either the ITER or DEMO, so an exact evaluation is needed, which is carried out using the Stokes polarization propagation equations [30, 32]. The values shown in table 10 are calculated including the relativistic corrections related to the plasma temperatures typical of the ITER and DEMO [31]. The theory derived in [32] was used.

5.2.2. Measurement of density by reflectometry and temperature by ECE (electron cyclotron emission). Microwave diagnostics like reflectometry and ECE with their need for reduced access, front-end robustness, space coverage, and spatial resolution are strong candidates to provide DEMO with measurements of electron density (reflectometry) and temperature profiles (ECEs) and *their associated fluctuations*. To evaluate the microwave accessibility to the plasma several DEMO1 scenarios were analyzed. The analysis was done assuming parameters for a DEMO1 model shown in table 1. Four snapshots, reflecting subsequent phases (at different times t1,t2, t3, t4) of a discharge, are included in the modelling: Figure 2 shows the density, magnetic field, and temperature spatial profiles used in the calculations reported in sections 5.2.2.1 (*evaluations of cut-offs and resonances for reflectometry*) and 5.2.2.2 (*evaluations for the spatial coverage of the ECE channels*). The profiles are obtained by METIS simulation of the DEMO1 discharge [33].

The main results can be summarized as follows:

(i) As shown in section 5.2.2.1, where the accessibility conditions of the waves are studied, the O-mode reflectometry (used for the measurements of plasma position and density spatial profile) can cover the plasma from edge to core both from the high and low field side with a set of frequencies ranging from 15–110 GHz. A low gradient at the plasma core can be a problem that could be magnified due to relativistic effects ($T_e > 2$ keV). For plasma position and shape control several poloidal views should be used with O-mode reflectometers probing the scrape-off layer. X-mode upper cut-off can be used to probe from the edge to core with frequencies ranging from 140–250 GHz. Due to relativistic effects the profile reconstruction depends on the knowledge of local T_e. There could also be conditions where large plasma regions are not accessible due to hollow or no gradient profile induced by peaked T_e profiles. The reflectometry does not need a first mirror close to the plasma, and waveguides are used.

(ii) For ECE (electron cyclotron emission, used for the measurement of electron temperature) some 40 channels ranging from 280 to 365 GHz using the X-mode electron cyclotron second harmonic will give electron temperature profiles with a spatial resolution of about 6 cm, very similar to what it is foreseen for the ITER.

The analysis was done assuming parameters for a DEMO1 model at different times of the discharge. In the analysis the relativistic effects must be also considered due to the fact that

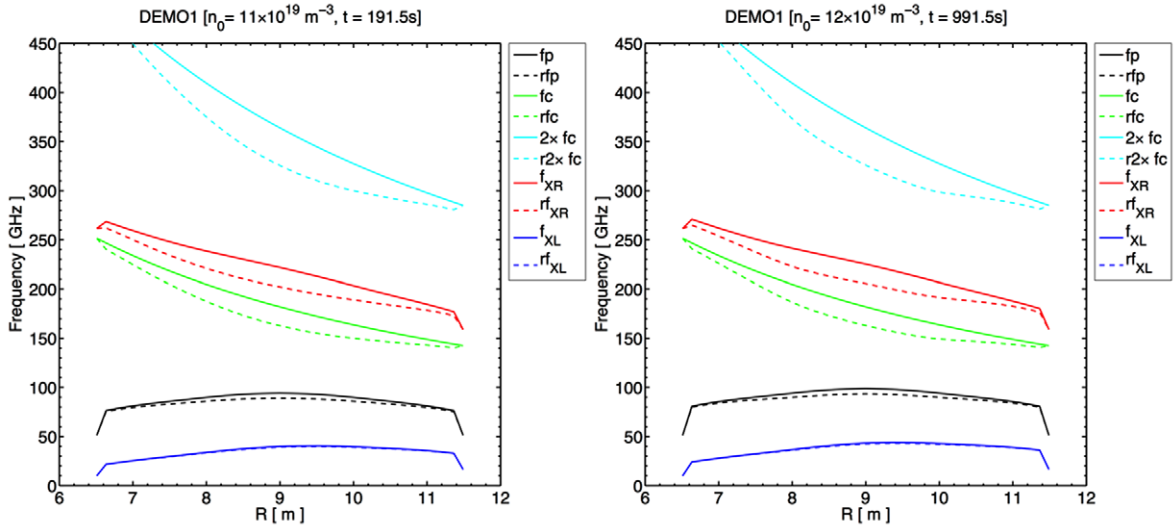

Figure 3. Cut-offs and resonances for the third (left) and fourth (right) scenarios. The dashed curves describe the dashed curved describe the resonances.

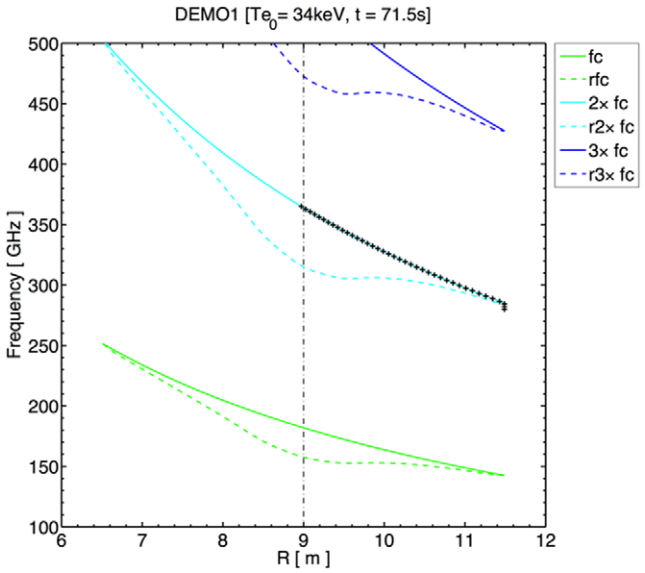

Figure 4. Spatial coverage and spatial resolution for the X-mode second harmonic ECE. The black crosses show the localization of the different channels.

the predicted electron temperatures are well above 2 keV. The effects include:

- Changes in the cut-off location.
- Hollow profiles or no gradient zones.
- The upper extraordinary mode (X_R) cut-off reflecting layers become strongly curved due to peaked T_e profiles.
- Absorption of microwave power at the relativistically downshifted second harmonic for ECE.

In consequence, the profile reconstruction will depend on the knowledge of the local electron temperature. The ordinary (O) and lower extraordinary mode (X_L) cut-offs are less affected. As explained in [34], the relativistic effects are the largest for the X-mode R-cut-off, the change in the critical density where the reflection happens increases by a factor two, while for L-cut-off and O-mode this change is definitely smaller.

The need to protect microwave based diagnostics from EM stray radiation, in particular from tens of MW of ECRH (coming from the heating systems) must be taken into account in the engineering design of these diagnostics (see section 5.2.2.3).

5.2.2.1. Reflectometry for plasma density and position control. The phases of the reflected O and X-mode waves contain information on the position of the reflecting plasma layer. To get this information for the X-mode waves we also need the magnetic field distribution. Measuring the phases on many different frequencies allows the reconstruction of the electron density profiles.

Figure 3 reports the cut-offs and resonances (dashed lines) for snapshots t3 and t4, at high plasma density.

Inspecting figure 3 on the black line related to the plasma frequency (fp), it is seen that O-mode reflectometry can cover the plasma from the edge to core both from the high and low field side with a set of frequencies ranging from 15–110 GHz, which gives a minimum density of 0.28×10^{19} m^{-3} and a maximum of 15×10^{19} m^{-3}. To probe smaller densities we need to use lower frequencies, which implies longer wavelengths with the resulting degradation of the measurements accuracy.

Real-time feedback control of the *plasma column position* is of vital importance for machine protection and preventing disruption. In present fusion devices this is done by using magnetic measurements. In the ITER, O-mode reflectometry was proposed to back up and complement the magnetic measurements. This new approach was successfully demonstrated for the first time on the ASDEX upgrade [35]. Due to the larger volume of the DEMO *for plasma position and shape control, many poloidal views with O-mode reflectometers* probing the scrape-off layer will be needed.

It should be also noted that due to the fact that a minimum density is indispensable for getting a reflection and corresponding measurement, it is impossible to provide control information during the very early plasma start-up phase, *an alternative scheme should be found for this period of the discharge.*

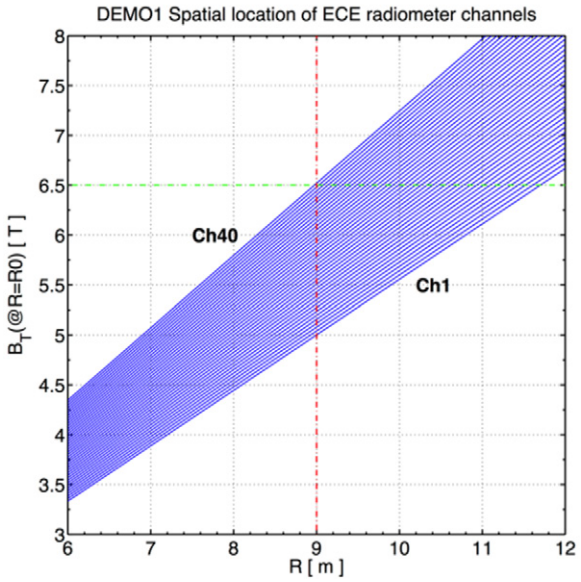

Figure 5. Spatial location of the ECE radiometer channels as a function of the toroidal field in DEMO1. The vertical dashed line represents the major radius and the horizontal dashed line represents the typical field $B_T = 6.5$ T.

5.2.2.2. ECE (electron cyclotron emission). The ECE diagnostic is expected to measure the electron temperature from the DEMO core, where the high temperature will be approximately 40 keV to the edge, where it could be as low as 0.05 keV.

To have a resolution of about 6 cm, similar to the one foreseen for the ITER ECE system [36], with the radius $a = 2.489$ m some 40 channels must be used in the range 280 to 365 GHz using the X-mode electron cyclotron second harmonic. The spatial coverage obtained with this arrangement is shown in figure 4, where the crosses show the locations of the various ECE channels.

A pseudo-radial displacement of the obtained electron temperature profile occurs if the relativistic frequency downshift effect is not taken into account in the determination of the emission layer position, see the dashed lines in figure 4. The shift could be a few centimeters as the electron temperature increases, and this effect should be taken into account.

The plasma coverage of the ECE radiometer channels as a function of toroidal field in DEMO is plotted in figure 5. The lines indicate the location of channels 1 (280 GHz) to 40 (365 GHz) when measuring the X-mode second harmonic.

If necessary, an *in situ* absolute calibration setup similar to the one proposed for the ITER ECE can be put in place. This allows the diagnostic to deliver independent temperature measurements despite the anticipated degradation of the front-end components.

5.2.2.3. EM stray field protection. The output power of modern gyrotrons is typically in the megawatt range with pulse lengths from several seconds to the CW. This means that even a small fraction of the total injected power has the potential to destroy millimeter wave diagnostics. The stray radiation can originate from non-perfect coupling to the plasma (e.g. wrong polarization of the injected millimeter wave beam), or reflections at plasma density cutoffs. There are also heating schemes with incomplete absorption of the injected millimeter wave power.

An excessive level of stray microwave power can lead to several diagnostic problems that range from signal corruption to more severe situations, where waveguide components arcing can occur or sensitive semiconductors can be burned due to their modest power handling capability (<100 mW), or in extreme situations the in-vessel components can be damaged due to thermal heating, which can also lead to outgassing and the release of impurities.

The most common protection techniques include the use of waveguide switches or shutters, PIN switches, band-pass or notch filters, waveguide isolators, and circulators.

Further R&D is critically needed in particular for the ECE systems. The frequency chirping during gyrotron start-up needs particular consideration.

5.2.3. Neutron measurements. There are only a limited number of physical parameters of neutrons that can be measured, namely the number of neutrons, the energy, and in certain detector systems the direction of the neutron. Depending on the plasma parameter to be measured, the time and spatial resolution targets may vary and will determine the diagnostic system and detector requirements.

Some of the main fusion neutron measurements are:

- Time-integrated neutron fluence that can be related to the fusion power output.
- Time-dependent neutron flux.
- Neutron energy, in particular the ratio of 2.5 Mev to 14.8MeV neutrons can be related to the fuel ion ratio.
- Time-dependent neutron flux as a function of spatial position, this can be combined with multiple measurements to make a tomographic reconstruction.
- A method of classifying diagnostics is by the parameters that are measured and if the diagnostic is the primary method of measuring a parameter, a backup/secondary method, or if it provides information that may useful in calculating a parameter but does not directly measure the parameter. This has been done for ITER diagnostics and the following table 11 is based on a longer and more detailed table presented by Bertalot [37]. The following short sections report comments on the diagnostic systems.

5.2.3.1. Fission chambers. In use in many fusion tokamaks around the world, and also used in accelerators and fission reactors for neutron production monitoring, fission chambers give time-resolved measurements of the neutron production rate and have previously been used in the JET as part of the control system. A choice of moderators can be fitted around the chamber to increase sensitivity or reduce count rates in high flux regions to avoid overloading the chamber. The fissile material can be either U235 or U238, and in most systems multiple chambers with different fissile contents are used to provide a small amount of neutron energy information. The U238 is sensitive to fast neutrons above about 1.45 MeV, whilst the U235 is sensitive across the energy range from thermal to very fast.

It is worth noting that due to the presence of fissile material extra safeguards need to be considered to ensure it cannot go missing. This may result in specific inspection requirements, which may impact the diagnostic system, control system, or remote handling system. The ITER will also face similar requirements and where possible the DEMO should use a similar system to the ITER.

5.2.3.2. Scintillation detectors (for neutron cameras). Scintillation detectors are an area of very active development with new types of scintillators appearing all the time, particularly for security and safeguard applications. The key areas of research appear to be improvements in the energy and time resolution as well as an improved ability to discriminate between gamma and neutron signals. There are both solid and liquid scintillation materials available from suppliers. The main issue for the DEMO will be the selection of appropriate scintillator and matching digital electronics.

A common scintillator detector used in many neutron producing physics experiments including the JET is NE213. It can be used as a spectrometer and time of flight system. There is over 15 years experience of using, calibrating, and maintaining NE213-based systems. Other scintillators that could be used for fusion neutron diagnostics include stilbene and modern organic plastic scintillators. Stilbene scintillators are used for fast neutron detection because of their strong capability of discrimination of neutron and gammas. Plastic scintillators under analysis as an alternative to NE213 are the EJ309 and EJ209-33 [38].

5.2.3.3. Application of scintillator detectors for gamma detection on the DEMO. Scintillators are relatively low-cost detectors that can be produced in large sizes to provide the efficient detection of gamma and hard x-ray radiation. During recent years the characterization of the most promising scintillator materials that can be considered as candidates for a gamma camera in the DEMO have been performed. A series of measurements have been performed in order to quantify crucial parameters like light output, non-proportionality, energy resolution, decay time, and peak detection efficiency in the gamma energy range of between 20 keV and 1.4 MeV. GAGG:Ce (one of the best choices of scintillators for semiconductor light readout). The results obtained during tests so far have indicated LaBr3:Ce, CeBr3 and GAGG:Ce as the most promising candidates for a gamma camera, although due to the fact that their response to intense neutron fluxes remains unknown, we find it necessary to extend the comparative study to all the above listed samples. One should keep in mind that high sensitivity to neutron radiation can exclude the best up-to-now choice of scintillators from the list of candidates for gamma monitoring, and may force the choice of material with somewhat worse characteristics, but less vulnerable to neutrons. The results of the tests devoted to a wider range of materials will also be very useful in the case of a need to search for another type of scintillator composed of elements that do not show sensitivity to intense neutron flux and can be synthesized in different configurations.

5.2.3.4. Activation foils. Activation foils are the standard method used to measure time integrated neutron flux, and with the correct selection of foils and use in unfolding techniques the neutron spectrum can be deduced. Typically they are used with a pneumatic transfer system to quickly move the foils from the irradiation position to the HPGe detector. Proposals for the ITER include a pneumatic transfer system for activation foils as a method for tritium breeding measurements in test breeding blanket modules. In that case, the foil selection is aimed at relatively short half life products so the count time can be minimized. The key limitations of activation foils are the lack of time-based data and the long count time, *they are therefore not suitable for plasma control purposes*. The measurements are, however, well-suited to neutron yield, tritium breeding, and radiation waste/dose assessment calculations, which are essential safety parameters. The accuracy of this method is mostly determined by the calibration of the system and the underlying nuclear data for the reactions used. When using foil activation techniques to determine the neutron spectrum the cross section data are used as part of the unfolding process to create response functions for each foil.

5.2.3.5. Micro-fission chambers. These are very similar to the normal fission chambers in terms of theory and operation, but instead of using shielding to reduce their sensitivity to high fluxes, a reduced fissile mass is used.

The micro-fission chambers to be used in the ITER as part of the neutron flux monitoring system were developed in Japan. There are current developments in Europe in this area particularly for TBM diagnostics, with the CEA in France currently developing a suitable system. There are a large number of papers covering everything from engineering design to detector response and prototype testing [39, 40]

5.2.3.6. Diamond detectors for neutron spectroscopy. Neutron spectroscopy plays an important role in the diagnosis of fusion processes in a tokamak. 14 MeV neutrons are emitted from the deuteitium-tritium (DT) reactions, and, having no charge, leave the tokamak and can be used to probe information on the confined ions energy and spatial distributions [41, 42].

The range of application of Single-crystal Diamond Detectors (SDDs) is expanding due to their wide-band-gap (5.5 eV), high radiation hardness, and high electron-hole mobility. These features, combined with the capability of performing neutron spectroscopy in environments with high temperatures and high magnetic fields, makes SDDs an interesting solution for neutron diagnostics in the DEMO, where the neutron fluxes will be very high. The SDD, being a very compact device ($4.5 \times 4.5 \times 0.5 mm^3$), allows also for simple integration into a camera system for neutron tomography measurements.

5.2.4. Magnetic sensors. The classification made in the ITER of magnetic sensors in-vessel and ex-vessel [43] cannot be translated to the DEMO, for the reason that (as saw for the first mirror) cables and sensors cannot survive in-vessel given the high level of damage (of the order of 10dpa on steel in one full power year on the first wall).

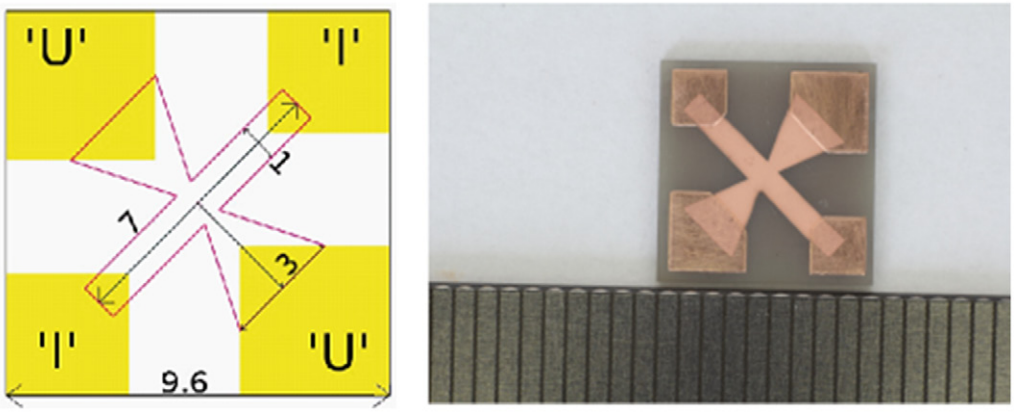

Figure 6. (a) Design of the Hall sensor (9.6 mm dimension). (b) Manufactured Hall sensor.

The effects of neutrons and gamma rays, the gradient of temperatures on components of magnetic sensors were analyzed for ITER magnetics and can be translated into the DEMO environment. Since the DEMO will have a higher neutron fluence and longer pulses with respect to the ITER, effects like RIC (radiation-induced conductivity in insulators), RIEMF (radiation-induced electromotive force in cables), TIEMF (thermally-induced electromotive-force), RITES (radiation-induced thermo-electric sensitivity), and RIED (radiation-induced electrical degradation) [17] will be even more important.

The research area of radiation-induced effects on cables and magnetic sensors for the DEMO, starting from the work done for the ITER, is an important R&D item for the DEMO.

The magnetic diagnostics are dedicated to (i) measurements of plasma current (by continuous external rogowski (CER) coils); (ii) magnetic flux for equilibrium reconstruction; (iii) halo current (this is a current flowing between the plasma and vacuum vessel) for disruption detection; (iv) MHD mode detection for magnetic instability reconstruction.

5.2.4.1. Measurement of plasma current. For the ITER Rogowski coil [43], a prototype was designed and tested. It is a long cable (20 m) surrounding the vacuum vessel and mounted in a groove cut in the casing of a TFC (toroidal field coil), and it will work at a temperature of 4.5 K.

Faraday rotation effect fiber optic current sensors (FOCS) for plasma current measurements are also considered for the ITER. The working principle of the Faraday fiber optic sensor is the following: The magnetic field H produced by the (plasma) current I, induces a birefringence in the fiber optic wrapped around a current, and this produces a Faraday rotation of the polarization of the light propagating inside the fiber. The Faraday rotation $\psi = \mu V{*}I$ is proportional to the current I and the Verdet constant, $\mu V = 0.7$ μrad/A or $1^\circ = >$ ~25 kA (silica), using an infrared light ($\lambda = 1500$ nm). Reference technical specifications for the FOCS parameters on the ITER can be: For plasma current 0–1 MA: Response time 10 ms, precision 10 kA; while for plasma current 1–20 MA: Response time 10 ms, precision 1%. FOCS tested on the Tore Supra tokamak were performed [44] in a ITER-like configuration to measure the plasma current. The reported measurements, performed using a laser at $\lambda = 1550$ nm and three types of fiber, demonstrate the capability of this method. One important output of the measurements was the measurements of the Verdet constant for the used fibers, in agreement with the expected value

$$\mu V = 0.71 \text{ rad/MA } \pm 6\%.$$

The effects of radiation (neutrons, gammas) [47] on the optical properties of silica can be grouped in the following list:

- Radiation-Induced Absorbtion (RIA) due to defect formation.
- Radiation-Induced Emission Luminescence (RIL), due to Photoluminescence and the Cherenkov effect in SiO2.
- Radiation-Induced Refractive Index Change (RIRIC).

RIA is usually the dominant effect to be taken into account in the integration of fibers in a radiative environment. Adverse effects of radiation and elevated temperatures on the life-time of optical fibers and possible mitigation strategies need to be examined in a *dedicated R&D programme*.

The possibility of using these two techniques in the DEMO for the measurement of plasma current must be assessed.

5.2.4.2. Magnetic measurements for equilibrium reconstruction. The conventional approach to magnetics includes the use of inductive sensors: To get the measurements of a magnetic field, a time integration is needed, and since the high neutron fluence results in spurious voltages generated inside the sensor, large errors can be made after integration on long pulses (400s pulses for ITER or ⩾2h pulses for the DEMO). *For this reason Hall sensors are considered where the integration is not needed.*

The R&D on Hall sensors for operation at high temperature and high neutron fluence is needed for ITER and DEMO applications.

Metallic Hall sensors seem to be the main candidate for magnetic sensors for the DEMO since intrinsically 'perturbative' diagnostics allowing ac detection in contrast to inductive loops, which are passive. The ability of Hall sensors to operate in an ac regime of operation removes most of the problems with thermoelectric and radiation-induced spurious voltages that are dc in nature, and which complicate operation of LTCC sensors already on the ITER.

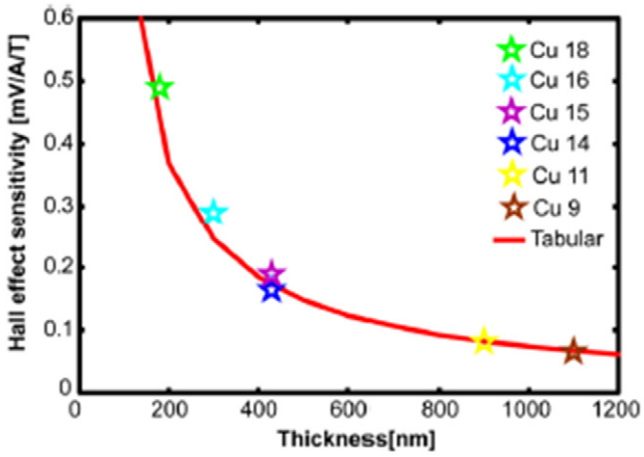

Figure 7. Sensitivity of the Cu Hall sensor versus the thickness of the sensing layer.

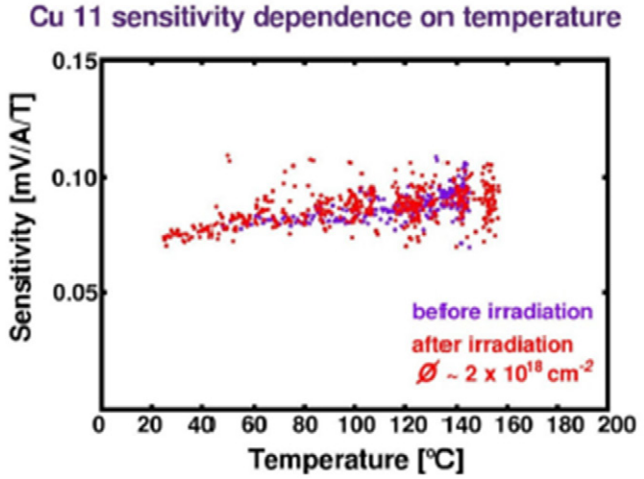

Figure 8. Temperature dependence of the intrinsic output noise.

The currently investigated technological solution includes a Direct Bond Copper (DBC) Al_2O_3 ceramic substrate 0.6 mm thick and a 127 μm thick layer of copper bonded on both sides (of the Al_2O_3 ceramic) [21].

The substrate of Al_2O_3 was chosen for practical purposes: It suffers from a 0.1–0.3% swelling at a fluence of 10^{24} neutron m^{-2}; for the application in the DEMO environment a substrate of Si_3N_4 can be a better choice since it is resistant to a fluence of 10^{26} neutron m^{-2}

Figures 6(a) and (b) (see also [21, 45, 46]) show the design of the Cu Hall sensor and the manufactured sensor (respectively): In figure 6(a) the 'I' contacts are used for the input voltage (bias), while the 'U' contacts are used for the output voltage. The measurement of the sensitivity (in the range of 0.1–0.5 mV A/T^{-1}) of these Hall sensors was carried out versus the thickness of the Cu sensing layer, and the results are shown in figure 7.

These sensors displayed a temperature dependence of the intrinsic output noise, as shown in figure 8: The measured temperature dependence of the output noise is shown for the Cu11 sensor (see figure 7) before and after neutron irradiation up to 2 10^{18} neutron cm^{-2}.

Reliable technology of metallic Hall sensors manufactured based on DBC substrates and possible for use in the DEMO environment has been developed. The copper Hall sensors showed a good neutron irradiation tolerance (tested up to 2×10^{18} cm^{-2}) and compatibility with elevated temperatures (tested up to 250 °C). Irradiation up to ~1×10^{19} cm^{-2} ($E > 0.1$ MeV) was done and analysis was underway.

5.3. Requirements on measurements for burn control

The analysis on the burn parameters (section 5.1) showed that the equilibrium temperature (T_{eq}) in the burning plasma depends mainly on the isotopic mix (f_{MIX}), dilution, radiation fraction ($C\alpha$), discharge geometry (V), and radiation fraction (krad).

To check the consistency of measurements, together with the previous measurements, three global parameters important for a burning plasma must be measured: (i) Temperature, (ii) fusion power, (iii) plasma density.

In section 5.2 a review of the diagnostics producing the measurements is presented.

In table 12 the requirements for the measurements based on the extrapolation to the DEMO of the present ITER requirements [17] and for the analysis of sections 5.1 and 5.2 are shown.

In table 12 the same space resolution adopted by the ITER measurements is retained, but the time resolution is relaxed by a factor 10. The electron temperature (T_e) is measured in the DEMO by ECE (Electron Cyclotron Emission). In the ITER the requirements for the Te spatial resolution is $\delta r = a/30 = 6.7$ cm, time resolution $=10^{-2}$ s, and accuracy $= 10\%$, (see table 12, red numbers).

The possibility of an accurate check on the temperature using Thomson scattering must be retained, so in the ILP Thomson scattering must be available to detect any discrepancy of electron temperature measurements between ECE and Thomson.

The accuracy set to 5% on the electron temperature on the DEMO is motivated by the necessity of doing a consistency check between Pfus_neut measured by the neutronics and Pfus_kin calculated from the kinetics, which will have the same accuracy. Clearly this objective ($\delta T_e/T_e \approx 5\%$) is a demanding performance for ECE and Thomson.

Measurements are needed to monitor the dilution, the isotopic mix, the radiation fraction, the burn equilibrium temperature, and the fast particle dynamics (see equation (4) section 5.1) and table 13 reports the related requirements for the measurements.

The measurement of plasma radiation in core, edge, and divertor plasma is an essential part of the plasma power balance, particularly for the DEMO (75% of the total input power to be irradiated): It includes the line radiation from the main impurities (W, Ar, N). The bolometers and VUV-soft x-ray spectroscopy are useful diagnostics for radiation measurements.

Table 13. Requirements for the additional measurements (RoM) for the diagnostics of DEMO burning plasma (in bold ITER RoM).

	Accuracy	Space resolution	Time resol(s)	Systems
Impurities (W,N,Ar)	10%(**10%**)	Integral	<0.1(**10 ms**)	VUV-x-ray spectroscopy
Radiated power	10%(**10%**)	Integral	<0.1(**10 ms**)	Bolometers
Zeff (line int.)	10%(**20%**)	Integral	<0.1(**10 ms**)	Vis spectroscopy
Confined fast ions	20%(**20%**)	Integral(**a/10**)	0.1(**0.1**)	NPA[a], γ-ray spectroscopy
nD/nT	≈10%(**20%**)	Integral(**a/10**)	0.1(**0.1**)	NPA
Ti(bulk)	10%(**10%**)	Integral (**a/10**)	0.1(**0.1**)	Neutronics, x-ray spectrometers

[a] Neutral particle analyzer.

Table 14. Actuator requirements for burn control.

Actuator	Plasma parameter controlled	Availability	Actuator output controlled	Latency [a]	Hardware response time
ECRH, NBI	Temperature and density profiles	All scenarios	Angle of ECRH launcher	<1 s	<1 s
ECRH, NBI, central solenoid	Conductivity profiles	Current rise	Angle of ECRH launcher	<1 s	<5 s
Impurity seeding (Ar,N)	Radiation profile (divertor detachment)	All scenarios	Impurity flux and density, Zeff (dilution, fusion power)	<0.1 s	<1 s
Deuterium gas injection	Density	All scenarios	Isotopic mix (fusion power)	<0.1 s	<1 s
Tritium (NBI or pellet)	Central fuelling	All scenarios	Isotopic mix (fusion power)	<1 s	<1 s
ECRH system	Parallel current	Steady state scenario	Angle of ECRH launcher	<1 s	<1 s
NBI	Plasma rotation	All scenarios, mainly steady state	NBI power	<1 s	<1 s
PF system	Plasma boundary	All scenarios	Higher moment of boundary shape or gap	<1 s	<1 s

[a] Maximum time delay from sensor input.

Using a tungsten first mirror and radiation hard bolometers (as developed for the ITER), placed in a recessed position (distance >1 m from first wall) is a possibility to be tested.

If this concept (tungsten mirrors and sensors placed in recessed positions) can also be applied to VUV-soft x-ray spectroscopy, and whether x-ray crystal spectroscopy to measure the ion temperature and visible continuum are open questions to be tested. The Zeff measurement is usually done by visible continuum in the region of the $\lambda = 500$–600 nm, this measurement is particularly important for burn control, because it is a dilution monitor.

All these measurements are made along a selected line of sight. The measurement requirement is a time resolution less than 100 ms: Since the confinement time is of the order of 1s, the MHD modes have a frequency of the order between 1–10 kHz, a reasonable time resolution can be 10 ms.

In the DEMO not many lines of sights can be available: A study is needed on the minimum number of measurements of radiation (including the divertor) optimized for input to the burn control.

The accuracy of measurements required in table 13 *is a reasonable compromise between the capability of the technology and the physics requirements*.

The measurements of the isotopic ratio (nD/nT) can be done using low-energy neutral particle analyzers (NPAs): The ITER NPA prototypes [48] were tested, and the declared accuracy and time resolution are given in table 13. These NPAs can also be candidates for DEMO, provided a direct line of sight to the plasma can be arranged. They can be arranged in a simplified version [48]. Taking advantage of the fact that the isotopic ratio D/T is not strongly dependent on the energy (in the MeV range), only two channels can be used one for D and two others for T ions. The high-energy NPA [48] can also be used for the measurements of knock-on D and T fast ion spectra resulting from collision with alpha particles. In this case the alpha particle energy distribution function could be extracted. The NPA detectors are not placed in the line of sight viewing the plasma [48], so they are not damaged from the neutrons coming directly from the plasma through the line of sight. The shielding of the detectors must be done taking into account the neutron fluence off the direct line of sight: In this case the plots in figures 1(a) and (b) can be helpful for defining the distance from the plasma and the shielding needed. R&D is needed to determine the engineering of the ITER NPA to be improved for application on the DEMO.

Table 15. Essential measurement, corresponding diagnostics, and control needs on the DEMO. The critical points of the diagnostics systems (where R&D is necessary) marked in bold.

Measurements	Control issue	Purpose	Diagnostic systems	Actuator
Plasma current	q95 limit	Disruption mitigation	Magnetic coils	Central solenoid/ current drive systems
Plasma density	Density limit	Burn control	Polarimetry, reflectometry	Gas valves/pellets/ pumping systems
Beta/density, temperature	Beta limit	Burn control	ECE, polarimetry, diamagnetic loop	ECRH, NBI, gas valves, pellet
Plasma position and shape	Vertical instability	MHD stability	Reflectometry, equilibrium (magnetic sensors)	PF/CS coils
Divertor heat flux	Limited wall load	Divertor control / detachment	Current/voltage measurement at divertor target, reflectometry, IR cameras, spectroscopy	PF coils/impurity seeding /impurity pellet/pumping system
Fusion power/fuel ion temperature; D/T ratio	Equilibrium Te stability	Real-time burn control	Neutron flux monitors, neutron camera/ neutron spectroscopy of tungsten for edge temperature/ Dα and Tα meas.	Deuterium/tritium, gas valves, impurity pellet/ heating systems, NBI
Radiated power; Zeff impurities	**Limited wall load, radiation collapse**	Real-time bun control	**Bolometers (R&D needed)/ spectroscopy**	Impurity seeding /pellet
Wall and blanket temperature	Material properties		**IR termography**	
Plasma instabilities	Disruptions	Disruption avoidance, ELM control/ mitigation	ECE polarimetry/magnetic sensors	ECCD/NBI
Plasma instabilities	Confinement / MHD stability	q-profile control (DEMO2 specific)	ECE polarimetry/magnetic sensors	ECCD/NBI
Runaway electrons	Damage to the first wall	Disruption mitigation	**IR termography, hard x-ray**	Pellet, gas valves
Confined Fast Ions	MHD stability/ Alfven waves	Burn control	NPA and gamma ray /magnetics	NBI, ECRH
Dust and tritium retention, lost fast ions	Damage to the first wall	Safety	**To be determined**	

The γ-ray spectroscopy can also be used to measure the fast ion energy distribution function in the region of energy > 1 MeV.

5.4. Actuators for burn control

The actuators for burn control are essentially gases and heating systems. Since the ratio $P_\alpha/P_{\text{Heating}}$ is high, the control by heating systems becomes less efficient (typically a control margin of the order of 30%) when entering the burn phase. Once the equilibrium temperature (T_{eq}) is reached, the control is done by fuelling, impurity seeding, isotopic mix, and radiation control, as noted in section 5.1 (formula (4)).

Table 14 shows the actuator requirements table for burn control (see also [18, 49]).

The burn control includes the following phases: (i) Current ramp and current profile optimization during ramp; (ii) burn initiation on flat top and temperature equilibrium optimization; (iii) current ramp down.

All these phases need pressure profile optimization and (for steady state DEMO2) current profile optimization.

A time scale sufficient for measurement is of the order of 10%* confinement time τE, since $\tau E = 3$–5 s the time resolution can be 100 ms or less (if possible); close loop feedback must act in a time below 0.8*τE; the space resolution of the sensors can be of the order of a/10–a/20, and accuracy of measurements the order of 10%. Most of the measurements are made in the lines of sight crossing the plasma.

During the current ramp, the pressure profile is controlled by a combined action of the ECRH and NBI, together with the transformer. The main fuelling tool is the NBI in this phase together with the gas valves. Once entering the burn phase at the flat top of the current, in a few confinement times the discharge will enter the burn phase, where the main objective is maintaining the optimized temperature or the burn, in the presence of the optimized radiation fraction.

In this phase the impurity seeding and gas valves are the main tool for the burn control, together with the deuterium and tritium gas valves. The main sensor for burn control is the neutron flux monitor (the neutron camera).

6. Essential measurements and candidate diagnostics for the DEMO

6.1. Diagnostics (likely) feasible (see table 15 for a summary) and guidelines for R&D

1. Reflectometry gives the measurement of the density profile at the edge and the pedestal and plasma position; ECE (electron cyclotron emission) the measurement of

electron temperature for bulk and edge plasma. They can be possible because small waveguides (WGs) to be used. The optimization of the dimensions of the ECE and reflectometry antenna must be done in conjunction with the achievement of TBR $\geqslant$ 1.1.
The WGs test to high fluences must be considered in the R&D programme.

2. Tangential polarimetry (TIP) and poloidal polarimetry (PoPola) [8]: Tungsten mirrors and retroreflectors in well-recessed positions (>1 m from the first wall) must be used in the PoPola as well as TIP systems well behind blanket. The test of this configuration for high neutron fluences must be checked. Far infrared lasers at a wavelength of $\lambda \geqslant 100$ μm can be used to get enough sensitivity for measuring Faraday rotation and Cotton–Mouton. In such systems relatively large dimension optics and beams are used, which must find a compromise with the requirement of the TBR $>$ 1 and related space limitations.
The tests of recrystallized tungsten mirrors at the DEMO fluences must be considered in the R&D programme.
3. Neutronics (including gamma-ray): The measurements of fusion power, fuel ion temperature, and confined alpha particles are used for burn control. The only neutron diagnostic linked to the control system on a tokamak is the total neutron flux; other plasma parameters derived from neutron measurements have not been linked to the control system.
The neutron diagnostics need a small tube-like access to be placed behind the shield. Difficult problems are related to the analysis of the signals and the absolute calibration. This area (absolute calibration) needs to be developed further if neutron diagnostics are to be used on the DEMO for control purposes.
4. Magnetics (metallic Hall sensors) can give the measurements of magnetic fluxes leading to the determination of the equilibrium. The necessity of placing the sensors behind the blanket likely will not spoil the high frequency measurements. Initial neutron irradiation tests of up to 2×10^{18} cm^{-2} showed no changes in sensitivity. The Rogowski coils projected for the ITER can be a starting point for the R&D on cable and sensors for DEMO. The Faraday rotation effect fiber optic current sensors (FOCS) for plasma current measurements are also considered for the ITER.
The dependence of sensitivity and the signal to noise ratio of the Hall sensors on the temperature must be further analyzed.
The magnetic sensors (Hall sensors as well as FOCs and cables) need to be tested at DEMO fluences. The possibility of replacing the sensors can also be considered.
5. First wall and divertor coolant temperature, flow and pressure give absolute measurements of the produced fusion power. The sensor is outside the machine; it has a low time resolution and no space resolution.
6. The current/voltage measurement at divertor target plates [15] is proportional to the plasma temperature at the divertor targets, so providing a monitoring of the divertor detachment. The possibility of mounting this system on the DEMO depends on the possibility of placing cables behind the divertor tiles.
This technique can be very useful and needs to be tested in a high fluence /high heat load environment.
7. Pressure and gas composition measurement in exhaust tube gives the *D/T ratio.*

6.2. Diagnostics important for the DEMO machine protection of difficult implementation

1. Infrared imaging (IR) monitors the integrity of the first wall and divertor. The IR cameras can measure the first wall and divertor temperature with a time resolution of 100 ms, a space resolution of the order of 7–10 mm, in the spectral range 3–5 μm. In the projects realized so far on the JET [50] and for the ITER [51], the optical design of the endoscope is usually quite delicate and involves many mirrors. The imaging properties of the first mirror (FM) will also depend on the capability of the *in situ* cleaning and surface protection of the FM using shutters. The RF cleaning technique was tested successfully on Mo mirrors in the context of a programme for the ITER first mirror development [52]. A 13.56 MHz radiofrequency source was used, and Ar as a gas for the plasma; the mirror becomes the antenna of the RF: It is cleaned using the plasma generated by the gas breakdown in front of the mirror. Polycrystalline molibdenum mirrors (98 mm diameter) were coated with aluminum of variable thickness of the order of 260 nm. This layer was removed after 130 h of discharge cleaning, restoring the pre-coating specular reflectivity. The cleaning tests were carried out in the presence of a magnetic field and also varying the angle of the mirror with respect to the magnetic field lines.
The possibility of mounting the FM on vertical ports for the divertor and first wall infrared imaging, can be beneficial for the FM because of the fluence being about 50% less than in equatorial ports.
A more refined version of the endoscope for IR viewing can include an extended spectral coverage to monitor impurities like W in the divertor [53].
IR imaging of the divertor and first wall using a first mirror mounted in a vertical port is a critical diagnostic for the machine protection; R&D is needed in this area to assess the possibility of building an IR viewing system for the DEMO.
2. Radiation measurements (bolometers and spectroscopy). The measurement of spatial distribution of radiation.
The bolometers enter the machine protection control table 3 related to disruptions and core/edge/divertor radiation control. The main role is to measure the radiation from visible to x-ray(20 keV), with the technical specifications defined in table 13. The range of power to be measured is Ptot $\approx$ 300 MW. The ITER design of the bolometers [54] is based on the resistive platinum absorber/SiN (silicium nitride)/platinum resistor. The design has been tested to 0.1dpa damage. Given the very close similarity of the atomic number and mass of platinum and tungsten, the same resistance of platinum and tungsten to neutron fluence can be expected. Following the same argument developed for the tungsten mirror position in section 3, these bolometers can suffer damage of 3dpa at 3 m

Table 16. Technology readiness level (TRL) and gap analysis.

Diagnostic system	TRL	R&D needed
Reflectometry /ECE	6	First Mirror/WGs tests
Polarimetry TIP/PoPola	6	Tungsten First mirror/retroreflectors to be tested
Neutron camera	6/5	CVD detectors/scintillators
Neutron flux	7	Fission chambers to be qualified
Gamma ray	5	Scintillators and neutron absorbers to be tested
Magnetics (equilibrium)	5	Metallic Hall sensors to be tested at DEMO fluence, signal-to-noise ratio versus temperature must be improved
Magnetics (plasma current)	4	Faraday rotation effects fiber (FOCS) and cables to be qualified for DEMO fluences
Measurement of Divertor detachment	4	The technique must be tested in a DEMO relevant environment
IR imaging	6	First mirror imaging properties to be tested / shutters / laser cleaning *in situ*
Bolometry	4	Radiation hard bolometers based on Pt absorbers to be tested at damage $>$ 0.1dpa; imaging bolometry concept must be tested for the DEMO environment
Erosion, dust, tritium retention	4	Various laser absorbtion and spectroscopy systems to be tested

from the first wall, mounted recessed in a tube with a pinhole looking directly to the plasma, and the electronics used must be radiation hardened. Bolometers placed at approximately 10 m from the first wall, in direct view of plasma, will suffer damage of the order of 0.3dpa, since the neutron flux will be approximately 1/10 (and then the damage will be 1/10) with respect to the position of 3 m from the first wall.

Another possibility is using imaging bolometers [55], which simply absorb platinum (Pt) foils 1–5 μm thick, whose temperature variation is measured by an infrared camera. The nuclear heating of the Pt Bolometer must be taken into account in the measurement; in this case two foils must be used, one of them shielded from radiation, to get the measurement of nuclear heating only. This geometry can be used also for the IR camera imaging system. Mounting the bolometers in the top part of the machine can be preferable (due to the reduced neutron flux with respect to the equatorial port); in this case the divertor bolometry can be arranged. *The bolometers are a key element where R&D must be done to ensure the resistance to damage of at least 0.1dpa, as well as the assembly of IR bolometry imaging.* Table 15 shows a summary of the essential measurements and control for the DEMO. The specific q-profile control is listed for DEMO2, the other controls are generic for both (DEMO1 and DEMO2).

3. Dust and tritium retention.

Laser-based diagnostics for determining the composition of the material of the wall and the tritium retention are being examined for the ITER [56]. The method is simply to heat by laser irradiation the surface and evaporate the material. When this irradiation is performed during the discharges, the material composition is determined by the spectroscopy of the emitted light when this material is decomposed and excited interacting with the plasma. These methods are laser-induced desorbtion spectroscopy (LIDS) and laser-induced ablation spectroscopy (LIAS). The ablation method can also be used between discharges, in this case the induced breakdown produces plasma which emits light, whose spectroscopy can give the amount of ablated species (LIBS).

The methods were tested on the TEXTOR requiring different laser pulses, but the same laser Nd:YAG. For LIDS, long pulses (tpulse = 1–3 ms, specific power 40 kW cm^{-2}) are used to heat up the wall at temperatures of the order of 2000 °K, and to let the hydrogen compounds be released by the wall. For the detection of hydrogen the laser-induced light can be seen only if it is higher then the Hα light emitted by the plasma. For example, in the TEXTOR a minimum flux of 10^{21} H atoms m^{-2} can be detected. For LIAS a higher specific power is needed like 140 MW cm^{-2} in 10 ns pulses for the ablation of a small layer. LIAS can be used to determine the thickness of the deposit and its composition.

These methods need to be demonstrated in dedicated R&D research programmes.

6.3. Important gaps and problems

6.3.1. Diagnostics systems. The analysis presented in section 6.1 can give some guide for defining the important gaps to be filled.

The necessity of testing methods for the measurement of the first wall erosion in the DEMO environment is one of the most important gaps to be filled by an R&D programme. This is also true for dust and tritium retention, *as well as bolometers*. Placing the magnetic sensors behind a blanket delays the detection of the signal; not changing its frequency content is a strong limit to the control. Tungsten first mirror damage tests at the DEMO relevant neutron fluences need to done. Alpha particle measurements, central to ITER operation, must be reconsidered for the DEMO.

Table 16 shows a first assessment of the technology readiness level (TRL, see appendix) of the diagnostics systems with R&D needs. The TRL can be a rough measure of the maturity of a system for the application on the DEMO. In general, a system cannot be TRL 9 until deployed and demonstrated on the DEMO, used on the JET typically represents around TRL 6 as it is a relevant environment and tested on a neutron source e.g. FNG (Frascati Neutron Generator) represents TRL 4.

Following the TRL classification, the ECE and reflectometry were tested on the JET (TRL6), but to be qualified for the DEMO the waveguides need to be tested at high neutron fluences for reflectometry, and for ECE the first mirror must also be qualified. The same arguments can be developed for the polarimetry PoPola and TIP, which were tested on the JET and JT60U (TRL6, respectively), but their application on the DEMO needs the first mirror and possibly the retroreflectors to be tested. The Hall sensors were tested in laboratory and their resistence under irradiation in fission reactors was determined (TRL5) but their use on the DEMO needs a dedicated development programme. The measurement of plasma current by Rogowski coils needs a specific test on the cables at DEMO fluences. This explains the evaluated TRL4. The test of FOC fibers at DEMO fluences needs to be done as well. The measurement of divertor detachment using current/voltage measurement on divertor target plates [15] was demonstrated on the AUG(TRL4), but needs to be demonstrated in the JET(TRL6) at least. The IR imaging system was demonstrated on the JET (TRL6); a similar concept is being developed for the ITER, where the first mirror and shutter need to be demonstrated. The bolometry using platinum sensors are tested at 0.1dpa damage (TRL4); they need to be tested for damage of the order of 0.3dpa. The measurements of tritium retention and wall erosion are at the level of laboratory development and demonstrated on a medium-sized tokamak device (TRL4).

Inspecting table 16 and looking at the TRL, some critical areas are identified where R&D is strongly needed: (i) Erosion, dust and tritium retention; (ii) bolometry; (iii) IR imaging; (iv) Faraday rotation effects fibers for plasma current measurements and cables, see sections 5 and 6.1 for an analysis of some of these systems. The ECE, polarimetry, and neutronics are in relatively better condition in the sense that some solutions are identified, and tests need to be organized. For example, the tungsten first mirrors are identified as a solution for the ITER, and (from neutronics calculations) it seems they can be a candidate for the DEMO. Tests are therefore required to demonstrate this conclusion at DEMO neutron fluences. The fission chambers are identified as an area where the current technology can be close to the solution useful for the DEMO. Regarding the bolometry and IR imaging, the evaluation is that the present solutions identified for the ITER must be evaluated for the DEMO, and their applicability for the DEMO is uncertain.

6.3.2. Control tools. The DEMO will have space for a few diagnostics, and the technology will be available for some valid implementation of a minimum set of sensors and actuators (see table 16). The experience before the DEMO must be used to construct an accurate model of the plasma. This model will be implemented in the ITER-like-phase of the DEMO, where an extended ITER-like set of sensors will be available. The implementation of control codes, including physics models inside and allowing for the safe extrapolations of the limited number of observations, is one of the main objectives of the research for the DEMO. This line of thought is developed in the context of the application of q-profile real-time control in the TCV [16]. The approach of the 'dynamic state observer' is used to predict in real time the q-profile to act on it using the ECCD. An important point to be realized is that the diagnostics observations available are used to constrain and improve the solution of a mathematical model of the plasma state. This tool can be used in various different contexts of plasma control like disruption avoidance, divertor control, and burn control. The planning of R&D must take into account that a program including the selection and testing of a minimum set of sensors and control schemes must be carried out on the ITER, JT-60SA, and other devices available before the DEMO comes into operation.

7. Conclusions

The perspective of diagnostics and control for the European DEMO is outlined in this paper. The first message emerging from the analysis is that DEMO diagnostics and controls should focus on high priority parameters useful for machine protection and burn control. The space available for diagnostics is severely limited by the Tritium Breeding Ratio (TBR), i.e. the space available is used by the blanket modules. The engineering of diagnostics must then be inserted in the overall DEMO design from the beginning, due to the optimization of the space dedicated, compatible with the TBR: Likely the organization of diagnostics in the PORT PLUGS adopted in the ITER and JT-60SA will not be used on the DEMO. The high fluence of the DEMO (30–50 $\times$ ITER fluence) put another important constraint on the diagnostics: In practice it is hard to think of mounting diagnostics components in-vessel. The general R&D issue is related to the radiation hardening of the diagnostics components: The first mirrors, components for magnetics, bolometry, IR viewing systems, and detectors for neutronics. The strategy for diagnostics and control optimization can be implemented in two phases: The ITER-like phase (ILP) and the power plant phase (PPP). The ILP is dedicated to the study of the control of a scenario with $Q > 10$ ($P_{alpha}/P_{heating} > 2$ (7(DEMO1); 2,4(DEMO2)). The external tools for the control of this scenario are limited (see sections 5.3 and 5.4), and the preparation of control using a limited set of diagnostics (like ECE, neutronics, polarimetry, and IR viewing) together with control codes is done in the ILP with an extended set of diagnostics similar to the ITER set, i.e. including profile diagnostics. The PPP will use a small set of diagnostics and actuators (see section 5.4). In this context the implementation of control codes, including the physics models inside and allowing for the safe extrapolation of the limited number observations, is one of the main objectives of the research for the DEMO. The R&D planning must take into account that a programme including the selection of tests of a minimum set of sensors and control schemes must be carried out on the ITER, JT-60SA, and other devices available before the DEMO comes into operation. Macro-areas where R&D is needed are related to (i) burn control, (ii) machine protection, (iii) general control codes, and (iv) radiation hardening of diagnostics components.

The analysis shows that there are critical areas and also encouraging results that have emerged related to (for example) the possible use of fission chambers as a candidate for DEMO

Table A1. Readiness level definitions.

TRL 1	Basic principles observed and reported.
TRL 2	Technology concept and/or application formulated.
TRL 3	Analytical and experimental critical function and/or characteristic proof-of-concept.
TRL 4	Technology basic validation in a laboratory environment.
TRL 5	Technology basic validation in a relevant environment.
TRL 6	Technology model or prototype demonstration in a relevant environment.
TRL 7	Technology prototype demonstration in an operational environment.
TRL 8	Actual technology completed and qualified through test and demonstration.
TRL 9	Actual technology qualified through successful mission operations.

neutron flux monitors or tungsten mirrors (already studied for the ITER), which are also candidates for first mirrors for the DEMO or metallic Hall sensors for magnetics.

Moderated efforts in R&D and the extrapolation from the ITER's presently considered technology can be dedicated to the infrared diagnostics (reflectometry, ECE) which use waveguides and are important for burn control, MHD stability, and basic machine protection. Neutron diagnostics can use CVD diamond detectors, candidate sensors for the ITER. The tungsten first mirror's resistence to high neutron fluences opens up the possibility of using the IR light for polarimetry measurements (density, equilibrium). Metallic Hall sensors are the main candidate for the magnetics for the DEMO and recent tests at high neutron fluences are encouraging. The analysis of diagnostics and control for the DEMO has given the great opportunity of looking in-depth into the future needs comparing that to the present status of the technology.

Acknowledgments

The study reported in this article was funded by EFDA under Task Agreement WP13-DAS04. The views and opinions expressed do not necessarily reflect those of the European Commission.

Appendix

Technology readiness level

The review of the diagnostic systems and detector technology provides evidence to try to quantify the current progress in diagnostics toward systems suitable for the DEMO. Technology readiness levels (TRLs) were developed by NASA, and are commonly used on major technology development programmes to measure progress, identify gaps, and reduce risks.

In general, a system cannot be TRL 9 until deployed and demonstrated on the DEMO; used on the JET typically it represents around TRL 6 as it is a relevant environment and tested on a neutron source e.g. FNG (Frascati Neutron Generator) it represents TRL 4. It should be noted that the first few TRLs are relatively easy to achieve, but it requires increased investment and development to go through the later levels, particularly in order to get closer and closer to the true environment. The definition of the TRLs is provided in table A1.

References

[1] Federici G. *et al* 2014 Overview of EU DEMO design and R&D activities *Fusion Eng. Des.* **89** 882–9
[2] Donne A.J.H., Costley A. and Morris W. 2012 Diagnostics for plasma control on DEMO: challenges of implementation *Nucl. Fusion* **52** 074015
[3] Orsitto F.P. *et al* 2014 *FINAL Report for Task Agreement WP13-DAS04,IDM* Reference: EFDA_D_2L4SFWv2.1 Date: 18.07.2014
[4] Gorini G. (ed) *et al* 2013 *Fusion Reactor Diagnostic Conf. AIP Proc. (Varenna, 9–13 September 2013)* vol 1612
[5] Wakatani M *et al* 1999 Plasma confinement and transport *Nucl. Fusion* **39** 2203
[6] Orsitto F.P. *et al* 2013 Diagnostics R&D for DEMO *IAEA 2nd DEMO Programme Workshop (Vienna, 2013)*
[7] Shimada M. *et al* 2007 ITER Physics basis *Nucl. Fus.* **47** S1–17
[8] Young K.M. 2010 Assessment of penetration in the first wall required for plasma measurements for controls of an advanced tokamak plasma DEMO *Sci. Tech.* **57** 298–304
[9] Todd T.N 2014 Diagnostics systems on DEMO:Engineering design issues *AIP Conf. Proc.* **1612** 9–16
[10] Pereslavtsev P. *et al* 2014 Neutronic analyses of the HCPB DEMO reactor using a consistent integral approach *Fusion Eng. Des.* **89** 1978–83
[11] Lu Z. *et al* 2009 *J. Nucl. Mater.* **386–388** 445–8
[12] Villari S. *et al* 2013 *Fusion Eng. Des.* **88** 2006–10
[13] Voitsenya V.S. *et al* 2013 Simulation of neutron influence on tungsten mirrors *Problems At. Sci. Technol.* **1** 64–6
[14] Palik E.D. 1985 *Handbook of Optical Constants of Solid* 2nd edn (New York: Academic)
[15] Litnovsky A. *et al* 2007 *J. Nucl. Mater.* **363–365** 1395–402
[16] Felici F. *et al* 2011 Real-time physics-model-based simulation of the current density profile in tokamak plasmas *Nucl. Fusion* **51** 083052
[17] Donne T. *et al* 2007 Progress in the ITER physics basis *Nucl. Fusion* **47** S337–84
[18] Snipes J. *et al* 2010 *Fusion Eng. Des.* **85** 461–5, ibidem 87(2012)1900–1906
[19] Kallenbach A. *et al* 2012 Divertor power load feedback with nitrogen seeding in ASDEX Upgrade *36th EPS Conf. on Plasma Physics (Sofia, June 29–July 3 2009) ECA vol 33 E, P-1.149)*; and *Nucl. Fusion* **52** 122003
[20] Felton R. 2014 Diagnostics for machine protection of DEMO *AIP Conf. Proc.* **1612** 17–22
[21] Duran I. *et al* 2014 Recent results and challenges in development of metallic hall sensors for fusion reactors *AIP Conf. Proc.* **1612** 31–4
[22] Petrov M. *et al* 2014 ITER diagnostics systems in development in Ioffe Institute *AIP Conf. Proc.* **1612** 188–93
[23] Shogunov I.N. *et al* 2011 Development of gamma-ray spectroscopy for ITER *Nucl. Fusion* **51** 083010
[24] Zohm H. 2013 Assessment of DEMO challenges in technology and physics *Fusion Eng. Des.* **88** 428
[25] Lackner K. 1994 *Comments Plasma Phys. Control. Fusion* **15** 359
[26] Wesson J. 1997 *Tokamaks* 2nd edn section1.7. (Oxford: Clarendon)

[27] Van Zeeland M. A. *et al* 2013 *Rev. Sci. Instrum.* **84** 043501
[28] Imazawa R. *et al* 2014 Multiparameter measurement utilizing poloidal polarimeter for burning plasma reactor *AIP Conf. Proc.* **1612** 61–8
[29] Kawano Y. *et al* 1999 *Rev. Sci. Instrum.* **70** 714
[30] Orsitto F.P. *et al* 2011 Analysis of Faraday rotation in JET polarimetric measurements *Plasma Phys. Control. Fusion* **53** 035001
[31] Mirnov V.V. *et al* 2014 Electron kinetic effects on interferometry, polarimetry, and Thomson scattering measurements in burning plasmas *Rev. Sci. Instrum.* **85** 11D302
[32] Segre S.E. 1978 The measurement of poloidal magnetic field in a tokamak by change of polarization of an electromagnetic wave *Plasma Phys.* **20** 295
[33] Giruzzi G. 2013 DEMO Physics assumptions and scenario modelling *IAEA 2nd DEMO Programme Workshop (Vienna, 2013)*
[34] Mazzucato E. 1992 Relativistic effects on microwave reflectometry *Phys. Fluids* **B4** 3460
[35] Santos J. *et al* 2012 *Nucl. Fusion* **52** 032003
[36] Rowan W. *et al* 2010 *Rev. Sci. Instrum.* **81** 10D935
[37] Bertalot L. 2005 Developments in neutron diagnostics during the JET trace tritium campaign *Fusion Eng. Des.* **74** 835–9
[38] Eriksson G. 2013 Recent advances in neutron and gamma ray diagnostics *Int. Conf. Fusion Reactor Diagnostics (Varenna, 9–13 september 2013)*
[39] Nishitani T. *et al* 1997 Design of ITER neutron yield monitor using microfission chambers *Fusion Eng. Des.* **34–35** 567–71
[40] Ishikawa M. *et al* 2008 Design of microfission chamber for ITER operations *Rev. Sci. Instrum.* **79** 10E507
[41] Tardocchi M. *et al* 2002 *Nucl. Fusion* **42** 1273
[42] Tardocchi M. *et al* 2011 *Phys. Res. Lab.* **107** 205002
[43] Vayakis G. *et al* 2012 *Rev. Sci. Instrum.* **83** 10D712
[44] Moreau Ph. *et al* 2013 *Fusion Eng. Des.* **88** 1165–9
[45] Kovafik K. *et al* 2013 *Fusion Eng. Des.* **88** 1319
[46] Sentkerestiova J. *et al* 2013 *Fusion Eng. Des.* **88** 1310
[47] Girard S. *et al* 2013 *IEEE Trans. Nucl. Sci.* **60** 2015
[48] Petrov M. *et al* 2014 ITER diagnostics systems in development in Ioffe Institute *AIP Conf. Proc.* **1612** 188–93
[49] Snipes J.A. *et al* 2014 *Fusion Eng. Des.* **89** 507–11 and ref. therein
[50] Clever M. *et al* 2012 *Fusion Eng. Des.* **88** 1342–6
[51] Reichle R. *et al* 2012 *Rev. Sci. Instrum.* **83** 10E520
[52] Leipold F. *et al* 2014 Cleaning of first mirror in ITER by means of RF discharges *ITER Report IDM UID KR4YA7* 22 September 2014
[53] Huber A. *et al* 2013 *Rev. Sci. Instrum.* **83** 10D511
Huber A. *et al* 2013 *Fusion Eng. Des.* **88** 1361–5
[54] Suarez A. *et al* 2013 *Fusion Eng. Des.* **88** 1395–9
[55] Peterson B.J. *et al* 2003 *Rev. Sci. Instrum.* **74** 2040
[56] Huber A. *et al* 2011 Development of laser-based diagnostics for surface characterization of wall components in fusion devices *Fusion Eng. Des.* **86** 1336
[57] Moreau D. *et al* 2003 Real tiem control of the q-profile in JET for steady state advanced tokamak operation *Plasma Phys. Control. Fusion* **43** 870–82
[58] Mazon D. *et al* 2003 Active control of current density profile in JET *Plasma Phys. Control. Fusion* **45** L47–54